Enhanced inhibition of the growth of* HER2 *amplification–positive gastric cancer cells* in vivo *by combined treatment with S-1 and either lapatinib or trastuzumab. Finally, we investigated the effect of combined treatment with S-1 and either lapatinib or trastuzumab on the growth *in vivo* of gastric cancer cells positive for *HER2* amplification. Mice with palpable tumors formed by NCI-N87 or 4-1ST cells were divided into groups for treatment with vehicle, S-1, lapatinib, trastuzumab, or the combination of S-1 and either lapatinib or trastuzumab

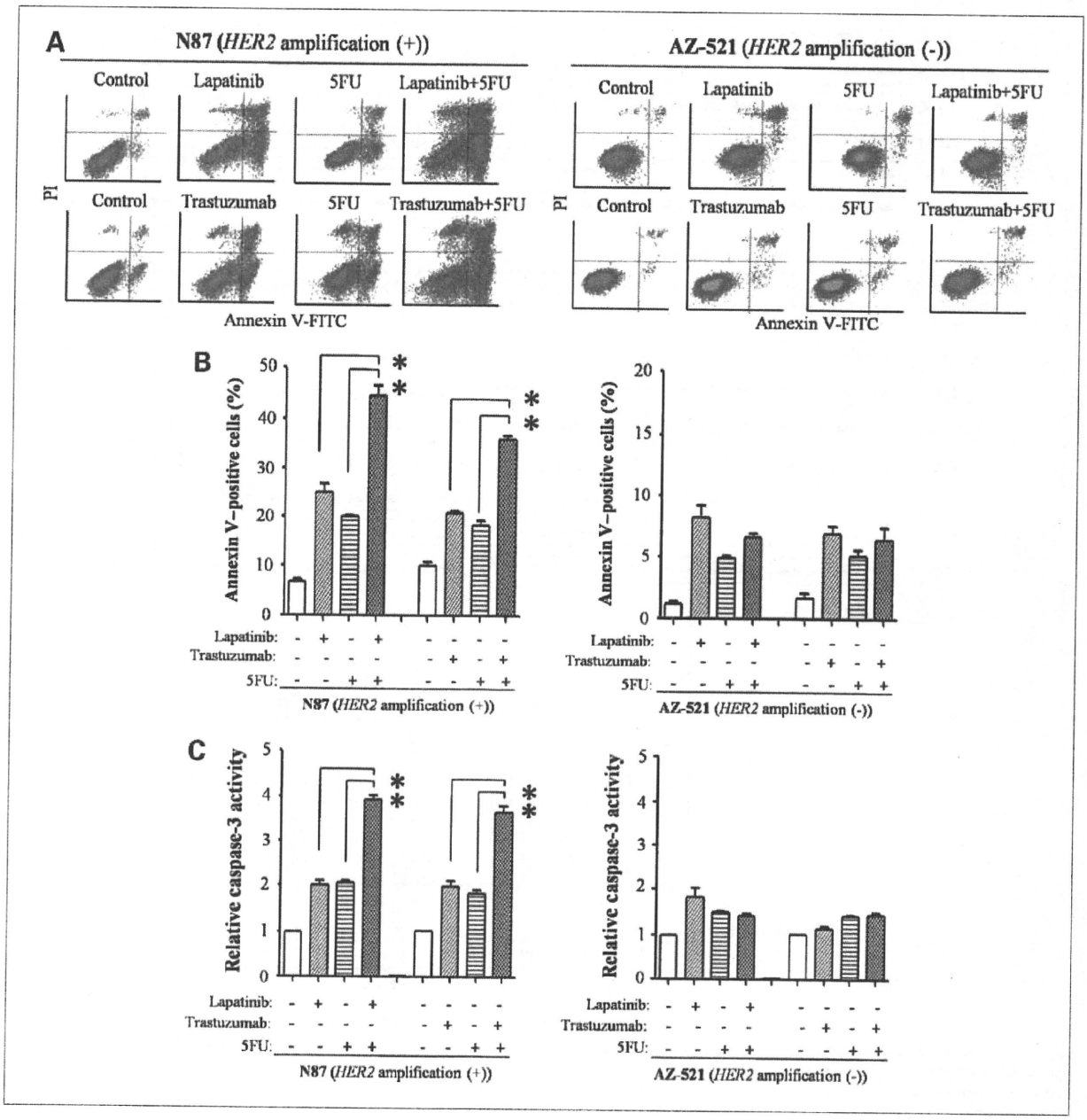

Figure 2. Effect of the combination of 5FU and HER2-targeting agents on apoptosis in gastric cancer cells positive or negative for *HER2* amplification. A, cells were incubated for 72 hours with lapatinib, trastuzumab, or 5FU at their IC_{50} concentrations unless indicated otherwise: 0.02 μmol/L, 1.5 μg/mL, and 2.5 μmol/L, respectively, for NCI-N87 cells and 2.0 μmol/L, 200 μg/mL (IC_{50} not determined), and 4.5 μmol/L, respectively, for AZ-521 cells. The proportion of apoptotic cells was then assessed by staining with FITC-conjugated Annexin V and propidium iodide (PI) followed by flow cytometry. B, the proportion of apoptotic cells in experiments similar to that shown in A was determined. Data are means ± SEM from three independent experiments. C, lysates prepared from cells exposed to drugs as in A for 48 hours were assayed for caspase-3 activity. Data are expressed relative to the corresponding value for the control condition and are means ± SEM from three independent experiments. *, $P < 0.05$, for the indicated comparisons.

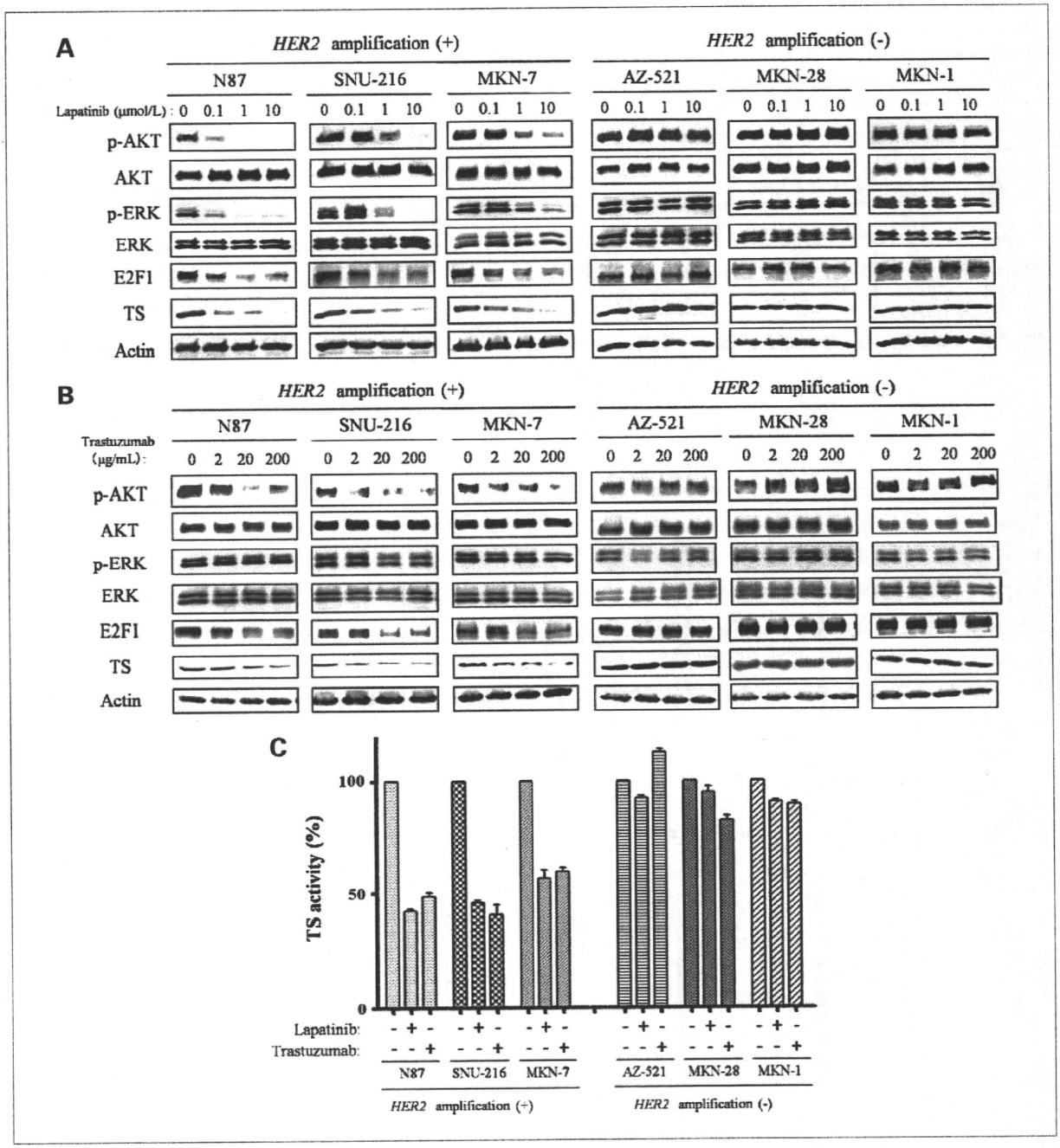

Figure 3. Effect of HER2-targeting agents on E2F1 and TS expression or activity in gastric cancer cells positive or negative for *HER2* amplification. A and B, cells were incubated with the indicated concentrations of lapatinib for 24 hours (A) or trastuzumab for 48 hours (B), after which cell lysates were prepared and subjected to immunoblot analysis with antibodies to phosphorylated (p) or total forms of AKT or ERK as well as with those to E2F1, TS, and β-actin (loading control). C, cells were treated with lapatinib (1 μmol/L) for 24 hours or with trastuzumab (200 μg/mL) for 48 hours, after which cell lysates were prepared and assayed for TS activity. Data are expressed as a percentage of the corresponding value for control cells and are means ± SEM from three independent experiments.

for 4 weeks. Combination therapy with S-1 and lapatinib (Fig. 5A) or with S-1 and trastuzumab (Fig. 5B) inhibited the growth of tumors formed by NCI-N87 or 4-1ST cells to a significantly greater extent than did treatment with either drug alone. All treatments were well tolerated by the mice, with no signs of toxicity or weight loss during therapy (data not shown). These findings thus suggested that combination therapy with S-1 and either lapatinib or

trastuzumab exhibits an enhanced antitumor effect in gastric cancer xenografts positive for *HER2* amplification, consistent with the results obtained *in vitro*.

Discussion

HER2 amplification is a frequent molecular abnormality in gastric cancer as well as in various other cancers. Trastuzumab is widely used as a standard therapy for HER2-positive patients with breast cancer, with the drug showing clinical efficacy both alone and in combination with chemotherapeutic agents (24, 25). HER2 is thus considered to be a potential target for the treatment of gastric cancer positive for *HER2* amplification. A recently reported phase III clinical trial showed a significant gain in overall survival for HER2-positive patients with advanced gastric cancer who received combined treatment with trastuzumab and fluoropyrimidine-cisplatin compared with those treated without trastuzumab (26). However, there has been limited examination of HER2-targeting agents in gastric cancer models, and most such studies have been restricted to cells with *HER2* amplification. Furthermore, the mechanisms of action of HER2-targeting agents in combination with cytotoxic agents have remained unclear.

In the present study, we have shown that the combination of S-1 (or 5FU) and HER2-targeting agents exerts a synergistic antitumor effect in gastric cancer cells with *HER2* amplification but not in those without it. We found that HER2-targeting agents inhibit TS activity as well as TS expression in *HER2* amplification–positive gastric cancer cells, but not in cells without *HER2* amplification. Lapatinib is a dual inhibitor of EGFR and HER2, and so its downregulation of TS might be attributable to inhibition of either of these tyrosine kinases. However, given that trastuzumab downregulated TS expression and activity to an extent similar to that observed with lapatinib, the effects of both lapatanib and trastuzumab on TS are likely mediated by inhibition of HER2. This conclusion is further supported by the observation that transfection of *HER2* amplification–positive gastric cancer cells with an siRNA specific for HER2 mRNA resulted in marked inhibition of TS expression, whereas transfection with an EGFR siRNA had no such effect (data not shown). Downregulation of TS by HER2-targeting agents was accompanied by a reduction in the abundance of E2F1, suggesting that this effect on TS results from attenuation of E2F1-dependent transcription of the TS gene. Although the mechanism responsible for regulation of TS and E2F1 remains unclear, our observations indicate that inhibition of the PI3K-AKT pathway contributes, at least in part, to the downregulation of TS by HER2-targeting agents. Activation of PI3K-AKT signaling has been found to result in E2F1 accumulation (27, 28), supporting the notion that inhibition of such signaling by HER2-targeting agents leads to downregulation of E2F1 and TS. We previously showed that inhibition of EGFR by EGFR–tyrosine kinase inhibitors results in downregulation of TS and E2F1

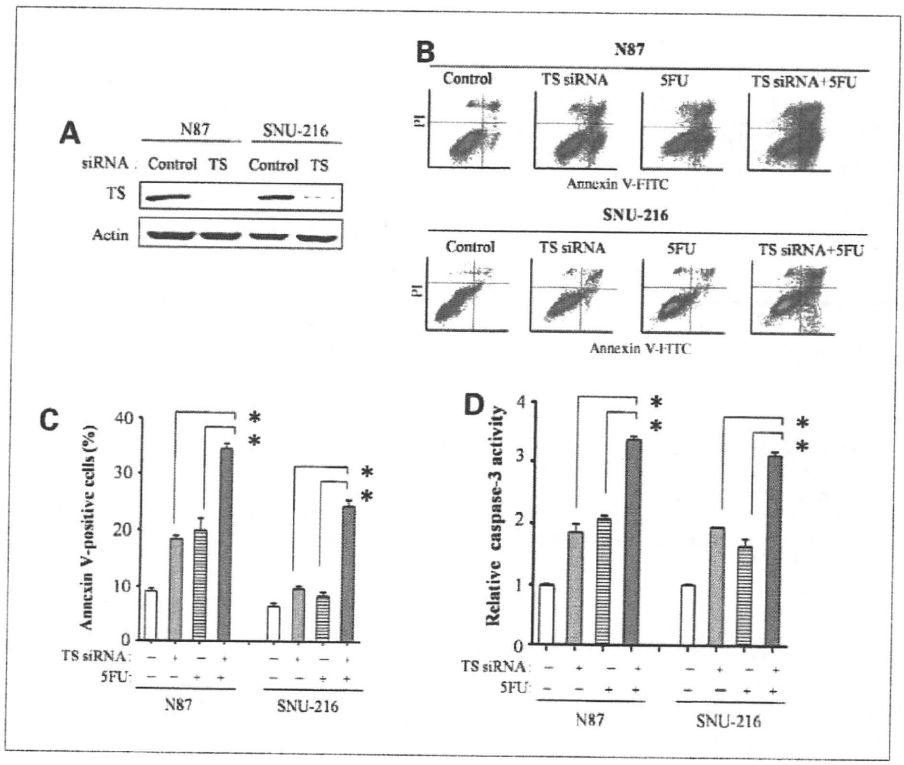

Figure 4. Effect of RNA interference–mediated depletion of TS on the proapoptotic action of 5FU in gastric cancer cells positive for *HER2* amplification. A, cells were transfected with nonspecific (control) or TS siRNAs for 48 hours, after which cell lysates were prepared and subjected to immunoblot analysis with antibodies to TS and to β-actin. B, cells were transfected with nonspecific or TS siRNAs as in A, replated and incubated for 72 hours in complete medium in the absence or presence of 5FU at IC_{50} concentrations (2.5 and 1.5 μmol/L for NCI-N87 and SNU-216 cells, respectively), and then evaluated for apoptosis by staining with Annexin V. C, the proportion of apoptotic cells in experiments similar to that in B was determined. Data are means ± SEM from three independent experiments. D, cells treated as in B were lysed and assayed for caspase-3 activity after exposure to 5FU for 48 hours. Data are means ± SEM from three independent experiments. *, $P < 0.05$ for the indicated comparisons.

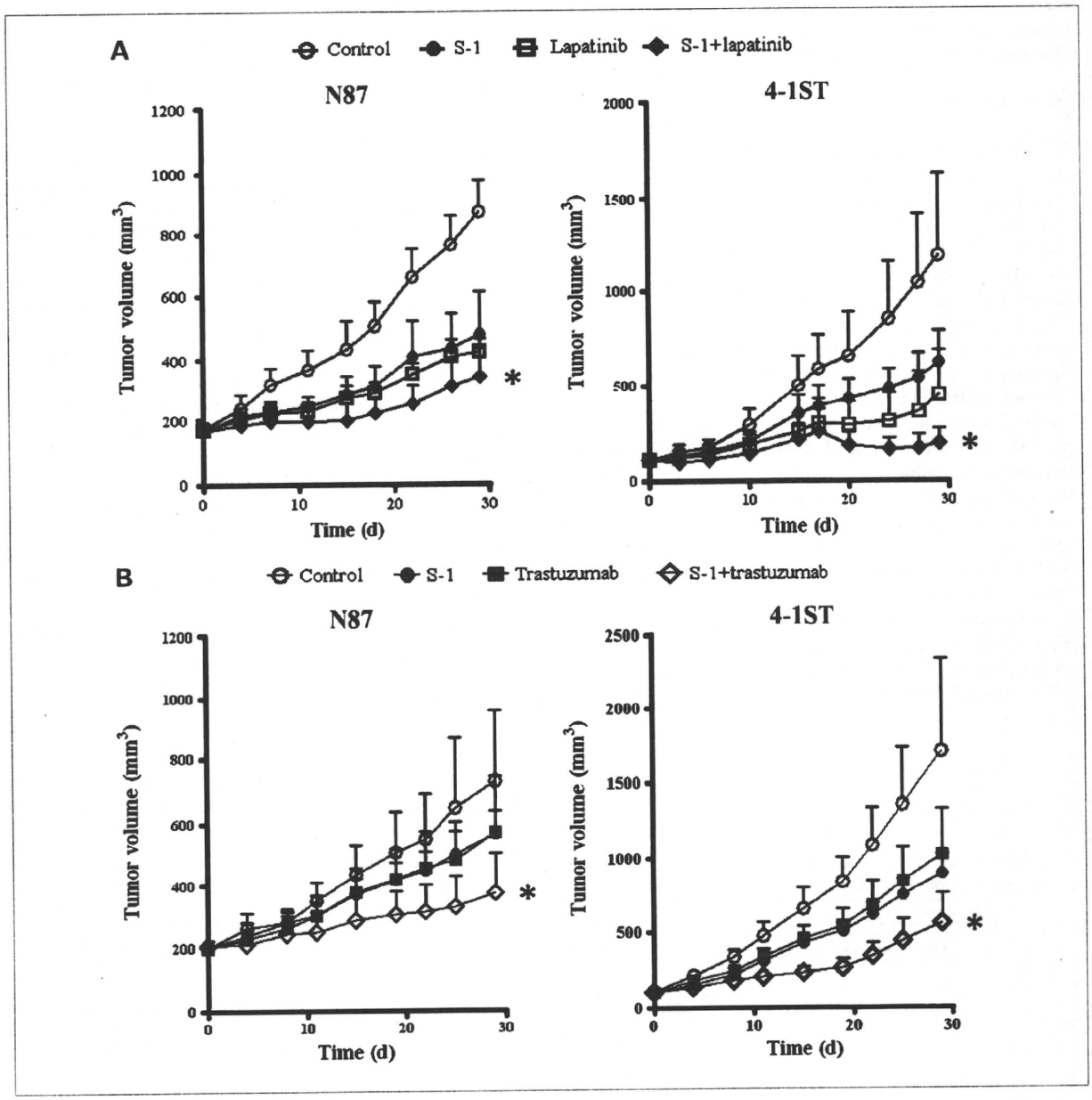

Figure 5. Effect of the combination of S-1 and HER2-targeting agents on the growth *in vivo* of gastric cancer cells with *HER2* amplification. Nude mice with tumor xenografts established by s.c. implantation of NCI-N87 cells were treated for 4 weeks by daily oral gavage with vehicle (control), S-1 (10 mg/kg), or lapatinib (50 × 2 mg/kg, twice a day; A) or by weekly i.p. administration of trastuzumab (20 mg/kg on days 1, 8, 15, and 22; B), as indicated. Nude mice with 4-1ST xenografts were similarly treated with vehicle (control), S-1 (8.3 mg/kg), lapatinib (30 × 2 mg/kg, twice a day; A), or trastuzumab (10 mg/kg on days 1, 8, 15, and 22; B). Tumor volume was determined at the indicated times after the onset of treatment. Data are means ± SEM of values from seven mice per group. *, $P < 0.05$, for the combination of S-1 plus lapatinib or trastuzumab at 28 days versus the corresponding value for S-1, lapatinib, or trastuzumab alone.

expression in non–small cell lung cancer cells (29, 30). Given that downregulation of TS was induced by HER2-targeting agents in gastric cancer cells with *HER2* amplification and by EGFR–tyrosine kinase inhibitors in non–small cell lung cancer cells, the expression of TS is likely dependent on receptor tyrosine kinase signaling, which is essential for cell survival.

Downregulation of TS expression has been found to enhance the efficacy of 5FU, possibly as a direct result of the decrease in the amount of this protein target of

5FU (31). In the present study, we found that depletion of TS by RNA interference enhanced the induction of apoptosis by 5FU in gastric cancer cells with *HER2* amplification, suggesting that the proapoptotic effect of the combination of 5FU and HER2-targeting agents is attributable to TS inhibition. The abundance of TS in neoplastic cells has been found to increase after exposure to 5FU, resulting in maintenance of the amount of the free enzyme in excess of that of enzyme bound to 5FU (32–34). Such an increase in TS expression and activity has been viewed as a mechanistic driver of 5FU resistance in cancer cells (22, 35–39). Downregulation of TS by HER2-targeting agents might thus contribute to reversal of the 5FU-induced increase in TS expression, resulting in enhancement of 5FU-induced apoptosis. In addition, prolonged inhibition of TS has been shown to trigger apoptosis by inducing an imbalance in the deoxyribonucleoside pool and consequent disruption of DNA synthesis and repair (40–42). Given that the TS siRNA itself induced apoptosis in gastric cancer cells positive for *HER2* amplification in the present study, the depletion of TS by HER2-targeting agents might also contribute directly to the combined proapoptotic action with 5FU.

The *HER2* amplification–positive gastric cancer cell line MKN-7 has been found to be insensitive to trastuzumab. In contrast to their insensitivity to trastuzumab, we found that MKN-7 cells retain sensitivity to lapatinib (IC_{50} values of >200 μg/mL and 0.99 ± 0.055 μmol/L for trastuzumab and lapatinib, respectively; data not shown). Most HER2-positive breast cancer patients who initially respond to trastuzumab ultimately develop resistance to this drug (25). Preclinical studies have indicated several molecular mechanisms that might contribute to the development of trastuzumab resistance, including signaling by a HER2-HER3-PI3K-PTEN pathway (43, 44). One possible explanation for trastuzumab resistance in MKN-7 cells is activation of the EGFR signaling pathway (45, 46). MKN-7 cells might prove to be a good model for the study of trastuzumab-resistant cells positive for *HER2* amplification. We found that lapatinib and trastuzumab each inhibit TS expression and activity in MKN-7 cells, likely accounting for the synergistic antiproliferative effect observed with 5FU. These data suggest that the synergistic antitumor effect of the combination of 5FU and HER2-targeting agents is conserved in trastuzumab-resistant cells with *HER2* amplification.

In conclusion, we have shown that the combination of S-1 and HER2-targeting agents exerts a synergistic antitumor effect mediated by TS inhibition in gastric cancer cells with *HER2* amplification, but not in those negative for *HER2* amplification. Our observations provide a rationale for clinical evaluation of combination chemotherapy with S-1 and HER2-targeting agents according to *HER2* amplification status.

Disclosure of Potential Conflicts of Interest

No potential conflicts of interest were disclosed.

Acknowledgments

We thank M. Iki for helpful discussion and E. Hatashita, K. Kuwata, and H. Yamaguchi for technical assistance.

The costs of publication of this article were defrayed in part by the payment of page charges. This article must therefore be hereby marked *advertisement* in accordance with 18 U.S.C. Section 1734 solely to indicate this fact.

Received 01/15/2010; revised 03/15/2010; accepted 03/17/2010; published OnlineFirst 04/27/2010.

References

1. Kelley JR, Duggan JM. Gastric cancer epidemiology and risk factors. J Clin Epidemiol 2003;56:1–9.
2. Kamangar F, Dores GM, Anderson WF. Patterns of cancer incidence, mortality, and prevalence across five continents: defining priorities to reduce cancer disparities in different geographic regions of the world. J Clin Oncol 2006;24:2137–50.
3. Hartgrink HH, Jansen EP, van Grieken NC, van de Velde CJ. Gastric cancer. Lancet 2009;374:477–90.
4. Wesolowski R, Lee C, Kim R. Is there a role for second-line chemotherapy in advanced gastric cancer? Lancet Oncol 2009;10:903–12.
5. Tatsumi K, Fukushima M, Shirasaka T, Fujii S. Inhibitory effects of pyrimidine, barbituric acid and pyridine derivatives on 5-fluorouracil degradation in rat liver extracts. Jpn J Cancer Res 1987;78:748–55.
6. Shirasaka T, Shimamato Y, Ohshimo H, et al. Development of a novel form of an oral 5-fluorouracil derivative (S-1) directed to the potentiation of the tumor selective cytotoxicity of 5-fluorouracil by two biochemical modulators. Anticancer Drugs 1996;7:548–57.
7. Sakata Y, Ohtsu A, Horikoshi N, Sugimachi K, Mitachi Y, Taguchi T. Late phase II study of novel oral fluoropyrimidine anticancer drug S-1 (1 M tegafur-0.4 M gimestat-1 M otastat potassium) in advanced gastric cancer patients. Eur J Cancer 1998;34:1715–20.
8. Koizumi W, Kurihara M, Nakano S, Hasegawa K. Phase II study of S-1, a novel oral derivative of 5-fluorouracil, in advanced gastric cancer. For the S-1 Cooperative Gastric Cancer Study Group. Oncology 2000;58:191–7.
9. Koizumi W, Narahara H, Hara T, et al. S-1 plus cisplatin versus S-1 alone for first-line treatment of advanced gastric cancer (SPIRITS trial): a phase III trial. Lancet Oncol 2008;9:215–21.
10. Sakuramoto S, Sasako M, Yamaguchi T, et al. Adjuvant chemotherapy for gastric cancer with S-1, an oral fluoropyrimidine. N Engl J Med 2007;357:1810–20.
11. Boku N. Chemotherapy for metastatic disease: review from JCOG trials. Int J Clin Oncol 2008;13:196–200.
12. Gravalos C, Jimeno A. HER2 in gastric cancer: a new prognostic factor and a novel therapeutic target. Ann Oncol 2008;19:1523–9.
13. Tanner M, Hollmen M, Junttila TT, et al. Amplification of HER-2 in gastric carcinoma: association with topoisomerase IIα gene amplification, intestinal type, poor prognosis and sensitivity to trastuzumab. Ann Oncol 2005;16:273–8.
14. Kim JW, Kim HP, Im SA, et al. The growth inhibitory effect of lapatinib, a dual inhibitor of EGFR and HER2 tyrosine kinase, in gastric cancer cell lines. Cancer Lett 2008;272:296–306.
15. Fujimoto-Ouchi K, Sekiguchi F, Yasuno H, Moriya Y, Mori K, Tanaka Y. Antitumor activity of trastuzumab in combination with chemotherapy in human gastric cancer xenograft models. Cancer Chemother Pharmacol 2007;59:795–805.
16. Kim HP, Yoon YK, Kim JW, et al. Lapatinib, a dual EGFR and HER2 tyrosine kinase inhibitor, downregulates thymidylate synthase by inhibiting the nuclear translocation of EGFR and HER2. PLoS One 2009;4:e5933.

17. Kim SY, Kim HP, Kim YJ, et al. Trastuzumab inhibits the growth of human gastric cancer cell lines with HER2 amplification synergistically with cisplatin. Int J Oncol 2008;32:89–95.
18. Wolff AC, Hammond ME, Schwartz JN, et al. American Society of Clinical Oncology/College of American Pathologists guideline recommendations for human epidermal growth factor receptor 2 testing in breast cancer. Arch Pathol Lab Med 2007;131:18–43.
19. Chou TC, Talalay P. Quantitative analysis of dose-effect relationships: the combined effects of multiple drugs or enzyme inhibitors. Adv Enzyme Regul 1984;22:27–55.
20. Spears CP, Gustavsson BG, Mitchell MS, et al. Thymidylate synthetase inhibition in malignant tumors and normal liver of patients given intravenous 5-fluorouracil. Cancer Res 1984;44:4144–50.
21. Johnston PG, Fisher ER, Rockette HE, et al. The role of thymidylate synthase expression in prognosis and outcome of adjuvant chemotherapy in patients with rectal cancer. J Clin Oncol 1994;12:2640–7.
22. Johnston PG, Drake JC, Trepel J, Allegra CJ. Immunological quantitation of thymidylate synthase using the monoclonal antibody TS 106 in 5-fluorouracil-sensitive and -resistant human cancer cell lines. Cancer Res 1992;52:4306–12.
23. DeGregori J, Kowalik T, Nevins JR. Cellular targets for activation by the E2F1 transcription factor include DNA synthesis- and G1/S-regulatory genes. Mol Cell Biol 1995;15:4215–24.
24. Cobleigh MA, Vogel CL, Tripathy D, et al. Multinational study of the efficacy and safety of humanized anti-HER2 monoclonal antibody in women who have HER2-overexpressing metastatic breast cancer that has progressed after chemotherapy for metastatic disease. J Clin Oncol 1999;17:2639–48.
25. Slamon DJ, Leyland-Jones B, Shak S, et al. Use of chemotherapy plus a monoclonal antibody against HER2 for metastatic breast cancer that overexpresses HER2. N Engl J Med 2001;344:783–92.
26. Van Cutsem E, Kang Y, Chung H. Efficacy results from the TOGA trial: a phase III study of trastuzumab added to standard chemotherapy (CT) in first-line human epidermal growth factor receptor 2 (HER2)-positive advanced gastric cancer (GC). J Clin Oncol 2009; 27:18s (abstr LBA4509).
27. Hallstrom TC, Nevins JR. Specificity in the activation and control of transcription factor E2F-dependent apoptosis. Proc Natl Acad Sci U S A 2003;100:10848–53.
28. Liu K, Paik JC, Wang B, Lin FT, Lin WC. Regulation of TopBP1 oligomerization by Akt/PKB for cell survival. EMBO J 2006;25:4795–807.
29. Okabe T, Okamoto I, Tsukioka S, et al. Addition of S-1 to the epidermal growth factor receptor inhibitor gefitinib overcomes gefitinib resistance in non-small cell lung cancer cell lines with MET amplification. Clin Cancer Res 2009;15:907–13.
30. Okabe T, Okamoto I, Tsukioka S, et al. Synergistic antitumor effect of S-1 and the epidermal growth factor receptor inhibitor gefitinib in non-small cell lung cancer cell lines: role of gefitinib-induced downregulation of thymidylate synthase. Mol Cancer Ther 2008;7:599–606.
31. Ferguson PJ, Collins O, Dean NM, et al. Antisense down-regulation of thymidylate synthase to suppress growth and enhance cytotoxicity of 5-FUdR, 5-FU and Tomudex in HeLa cells. Br J Pharmacol 1999;127:1777–86.
32. Washtien WL. Increased levels of thymidylate synthetase in cells exposed to 5-fluorouracil. Mol Pharmacol 1984;25:171–7.
33. Spears CP, Gustavsson BG, Berne M, Frosing R, Bernstein L, Hayes AA. Mechanisms of innate resistance to thymidylate synthase inhibition after 5-fluorouracil. Cancer Res 1988;48:5894–900.
34. Chu E, Zinn S, Boarman D, Allegra CJ. Interaction of γ interferon and 5-fluorouracil in the H630 human colon carcinoma cell line. Cancer Res 1990;50:5834–40.
35. Copur S, Aiba K, Drake JC, Allegra CJ, Chu E. Thymidylate synthase gene amplification in human colon cancer cell lines resistant to 5-fluorouracil. Biochem Pharmacol 1995;49:1419–26.
36. Chu E, Koeller DM, Johnston PG, Zinn S, Allegra CJ. Regulation of thymidylate synthase in human colon cancer cells treated with 5-fluorouracil and interferon-γ. Mol Pharmacol 1993;43:527–33.
37. Chu E, Voeller DM, Jones KL, et al. Identification of a thymidylate synthase ribonucleoprotein complex in human colon cancer cells. Mol Cell Biol 1994;14:207–13.
38. Longley DB, Harkin DP, Johnston PG. 5-Fluorouracil: mechanisms of action and clinical strategies. Nat Rev Cancer 2003;3:330–8.
39. Kawate H, Landis DM, Loeb LA. Distribution of mutations in human thymidylate synthase yielding resistance to 5-fluorodeoxyuridine. J Biol Chem 2002;277:36304–11.
40. Yoshioka A, Tanaka S, Hiraoka O, et al. Deoxyribonucleoside triphosphate imbalance. 5-Fluorodeoxyuridine-induced DNA double strand breaks in mouse FM3A cells and the mechanism of cell death. J Biol Chem 1987;262:8235–41.
41. Ayusawa D, Shimizu K, Koyama H, Takeishi K, Seno T. Accumulation of DNA strand breaks during thymineless death in thymidylate synthase-negative mutants of mouse FM3A cells. J Biol Chem 1983;258:12448–54.
42. Wyatt MD, Wilson DM III. Participation of DNA repair in the response to 5-fluorouracil. Cell Mol Life Sci 2009;66:788–99.
43. Kruser TJ, Wheeler DL. Mechanisms of resistance to HER family targeting antibodies. Exp Cell Res 2010;316:1083–100.
44. Nahta R, Yu D, Hung MC, Hortobagyi GN, Esteva FJ. Mechanisms of disease: understanding resistance to HER2-targeted therapy in human breast cancer. Nat Clin Pract Oncol 2006;3:269–80.
45. Lane HA, Beuvink I, Motoyama AB, Daly JM, Neve RM, Hynes NE. ErbB2 potentiates breast tumor proliferation through modulation of p27(Kip1)-Cdk2 complex formation: receptor overexpression does not determine growth dependency. Mol Cell Biol 2000;20: 3210–23.
46. Lewis GD, Figari I, Fendly B, et al. Differential responses of human tumor cell lines to anti-p185HER2 monoclonal antibodies. Cancer Immunol Immunother 1993;37:255–63.

Research Article

Molecular Cancer Therapeutics

Identification of c-Src as a Potential Therapeutic Target for Gastric Cancer and of MET Activation as a Cause of Resistance to c-Src Inhibition

Wataru Okamoto[1], Isamu Okamoto[1], Takeshi Yoshida[1], Kunio Okamoto[1], Ken Takezawa[1], Erina Hatashita[1], Yuki Yamada[1], Kiyoko Kuwata[1], Tokuzo Arao[2], Kazuyoshi Yanagihara[4], Masahiro Fukuoka[3], Kazuto Nishio[2], and Kazuhiko Nakagawa[1]

Abstract

Therapeutic strategies that target c-Src hold promise for a wide variety of cancers. We have now investigated both the effects of dasatinib, which inhibits the activity of c-Src and several other kinases, on cell growth as well as the mechanism of dasatinib resistance in human gastric cancer cell lines. Immunoblot analysis revealed the activation of c-Src at various levels in most gastric cancer cell lines examined. Dasatinib inhibited the phosphorylation of extracellular signal-regulated kinase (ERK) and induced G_1 arrest, as revealed by flow cytometry, in a subset of responsive cell lines. In other responsive cell lines, dasatinib inhibited both ERK and AKT phosphorylation and induced apoptosis, as revealed by an increase in caspase-3 activity and cleavage of poly(ADP-ribose) polymerase. Depletion of c-Src by RNA interference also induced G_1 arrest or apoptosis in dasatinib-responsive cell lines, indicating that the antiproliferative effect of dasatinib is attributable to c-Src inhibition. Gastric cancer cell lines positive for the activation of MET were resistant to dasatinib. Dasatinib had no effect on ERK or AKT signaling, whereas the MET inhibitor PHA-665752 induced apoptosis in these cells. The subsets of gastric cancer cells defined by a response to c-Src or MET inhibitors were distinct and nonoverlapping. Our results suggest that c-Src is a promising target for the treatment of gastric cancer and that analysis of *MET* amplification might optimize patient selection for treatment with c-Src inhibitors. *Mol Cancer Ther; 9(5); 1188–97. ©2010 AACR.*

Introduction

Gastric cancer is the second most frequent cause of cancer deaths worldwide (1). Chemotherapy has a beneficial effect on survival in individuals with advanced-stage gastric cancer, but overall survival is still usually <1 year (1, 2). Advanced gastric cancer is treated predominantly with the combination of fluoropyrimidine derivatives and platinum compounds, although a globally accepted standard regimen remains to be established. Improved therapy for affected individuals is thus urgently needed.

Authors' Affiliations: Departments of [1]Medical Oncology and [2]Genome Biology, Kinki University School of Medicine, 377-2 Ohno-higashi, Osaka-Sayama; and [3]Department of Medical Oncology, Kinki University School of Medicine, Sakai Hospital, 2-7-1 Harayamadai, Minami-ku Sakai, Osaka, Japan; and [4]Laboratory of Health Sciences, Department of Life Sciences, Yasuda Women's University Faculty of Pharmacy, 6-13-1 Yasuhigashi, Asaminami, Hiroshima, Japan

Note: Supplementary material for this article is available at Molecular Cancer Therapeutics Online (http://mct.aacrjournals.org/).

Corresponding Author: Isamu Okamoto, Department of Medical Oncology, Kinki University School of Medicine, 377-2 Ohno-higashi, Osaka-Sayama, Osaka 589-8511, Japan. Phone: 81-72-366-0221; Fax: 81-72-360-5000. E-mail: chi-okamoto@dotd.med.kindai.ac.jp

doi: 10.1158/1535-7163.MCT-10-0002

c-Src is a nonreceptor tyrosine kinase that plays key roles in intracellular signaling by interacting with and phosphorylating multiple proteins and protein complexes (3). Activation of c-Src has been found to contribute to the transformation, proliferation, survival, and motility of malignant cells as well as to tumor angiogenesis (3, 4). c-Src is highly activated in a wide variety of human cancers and clinical studies have shown that such aberrant activation is correlated with malignant progression (5). These properties have rendered c-Src a potential target for the treatment of solid tumors.

Dasatinib is an oral, multitargeted inhibitor of tyrosine kinases that inhibits the activities of c-Src, Bcr-Abl, and other kinases (6). It has been approved for clinical use in patients with chronic myelogenous leukemia or Philadelphia chromosome–positive acute lymphoblastic leukemia and it is currently under investigation as a potential therapy for solid tumors. Recent studies have shown that c-Src inhibitors induce apoptosis or arrest cell cycle progression in various cancer cell types (7–14). The activation of c-Src has pleiotropic effects that depend on cell type and context. Although c-Src activity has been found to be increased in most gastric cancers (15–18), the responses of gastric cancer cells to c-Src inhibition have not previously been characterized. We have therefore now examined the effects of c-Src inhibition by

dasatinib on cell growth and signal transduction in human gastric cancer cell lines. Furthermore, we have investigated the mechanism of resistance to dasatinib in such cells. Our results provide a rationale for the clinical investigation of c-Src inhibition in individuals with gastric cancer.

Materials and Methods

Cell culture and reagents. The human gastric cancer cell lines SNU1, SNU5, Hs746T, and AGS were obtained from the American Type Culture Collection; MKN1, MKN7, MKN45, NUGC3, and AZ521 were from the Health Science Research Resources Bank; OKAJIMA, MKN28, and HSC39 were from Immuno-Biological Laboratories; and SNU216 was from the Korean Cell Line Bank. HSC58, 58As1, and 58As9 are established cell lines derived from human scirrhous gastric carcinoma as previously described (19). All cells were cultured under a humidified atmosphere of 5% CO_2 at 37°C in RPMI 1640 (Sigma,) supplemented with 10% fetal bovine serum and were passaged for ≤3 mo before the renewal from frozen, early-passage stocks obtained from the indicated sources. Cells were regularly screened for *Mycoplasma* with the use of a MycoAlert Mycoplasma Detection kit (Lonza). Dasatinib was kindly provided by Bristol-Myers Squibb and PHA-665752 was obtained from Tocris Bioscience.

Immunoblot analysis. Cells were washed twice with ice-cold PBS and then lysed with 1× Cell Lysis Buffer (Cell Signaling Technology) containing 20 mmol/L Tris-HCl (pH 7.5), 150 mmol/L NaCl, 1 mmol/L EDTA (disodium salt), 1 mmol/L EGTA, 1% Triton X-100, 2.5 mmol/L sodium pyrophosphate, 1 mmol/L β-glycerophosphate, 1 mmol/L Na_3VO_4, leupeptin (1 μg/mL), and 1 mmol/L phenylmethylsulfonyl fluoride. The protein concentration of cell lysates was determined with a BCA protein assay kit (Thermo Fisher Scientific) and equal amounts of protein were subjected to SDS-PAGE on 7.5 or 12% gels (Bio-Rad). The separated proteins were transferred to a nitrocellulose membrane, which was then incubated with Blocking One solution (Nacalai Tesque) for 20 minutes at room temperature before incubation overnight at 4°C with primary antibodies. Antibodies to phosphorylated c-Src (Y416), total c-Src, phosphorylated MET (Y1234/1235, Y1349), phosphorylated AKT, total AKT, phosphorylated extracellular signal-regulated kinase (ERK), p27, or poly (ADP-ribose) polymerase (PARP) were obtained from Cell Signaling Technology; those to total ERK were from Santa Cruz Biotechnology; those to total MET were from Zymed/Invitrogen; and those to β-actin were from Sigma. The membrane was then washed with PBS containing 0.05% Tween 20 before incubation for 1 h at room temperature with horseradish peroxidase–conjugated antibodies to rabbit or mouse IgG (GE Healthcare). Immune complexes were finally detected with enhanced chemiluminescence (Amersham) Western Blotting Detection Reagents (GE Healthcare).

Cell growth inhibition assay. Cells were transferred to 96-well flat-bottomed plates and cultured for 24 hours before exposure to various concentrations of dasatinib or PHA-665752 for 72 hours. Tetra Color One (5 mmol/L tetrazolium monosodium salt and 0.2 mmol/L 1-methoxy-5-methyl phenazinium methylsulfate; Seikagaku Kogyo) was then added to each well and the cells were incubated for 3 hours at 37°C before measurement of absorbance at 490 nm with a Multiskan Spectrum instrument (Thermo Labsystems). Absorbance values were expressed as a percentage of that for nontreated cells and the concentration of dasatinib resulting in 50% growth inhibition (IC_{50}) was calculated.

Fluorescence* in situ *hybridization analysis. *MET* gene copy number per cell was determined by fluorescence *in situ* hybridization with the use of the LSI D7S522 (7q31) Spectrum Orange and chromosome 7 centromere (CEP7) Spectrum Green probes (Vysis; Abbott). Cells were centrifuged onto glass slides with a Shandon cytocentrifuge (Thermo Electron) and were fixed by consecutive incubations with ice-cold 70% ethanol for 10 minutes, 85% ethanol for 5 minutes, and 100% ethanol for 5 minutes. Slides were stored at −20°C until analysis. Cells were subsequently subjected to digestion with pepsin for 10 minutes at 37°C, washed with water, dehydrated with a graded series of ethanol solutions, denatured with 70% formamide in 2× SSC for 5 minutes at 72°C, and dehydrated again with a graded series of ethanol solutions before incubation with a hybridization mixture consisting of 50% formamide, 2× SSC, Cot-1 DNA, and labeled DNA. The slides were washed for 5 minutes at 73°C with 3× SSC, for 5 minutes at 37°C with 4× SSC containing 0.1% Triton X-100, and for 5 minutes at room temperature with 2× SSC before counterstaining with an antifade solution containing 4′,6-diamidino-2-phenylindole. Hybridization signals were scored in 40 nuclei with the use of a ×100 immersion objective lens. Nuclei with a disrupted boundary were excluded from the analysis. Gene amplification was defined by a mean *MET*/chromosome 7 copy number ratio of >2.2 or by a mean *MET* copy number of >6 per cell, corresponding to the previous definition for *HER2* amplification (20).

Cell cycle analysis. Cells were harvested, washed with PBS, fixed with ice-cold 70% methanol, washed again with PBS, and stained with propidium iodide–RNase staining buffer (BD Biosciences) for 15 minutes at room temperature. The stained cells were then analyzed for DNA content with a flow cytometer (FACSCalibur, BD Biosciences) and the Modfit software (Verity Software House).

Assay of caspase-3 activity. The activity of caspase-3 in cell lysates was measured with a CCP32/Caspase-3 Fluometric Protease Assay kit (Medical Biological Laboratories). Fluorescence attributable to the cleavage of the Asp-Glu-Val-Asp-7-amino-4-trifluoromethyl coumarin (DEVD-AFC) substrate was measured at excitation and emission wavelengths of 390 and 460 nm, respectively.

Gene silencing. Cells were plated at 50% to 60% confluence in six-well plates or 25-cm^2 flasks and were incubated for 24 hours before transient transfection with small interfering RNAs (siRNA) for 48 or 72 hours with the use of the Lipofectamine RNAiMAX reagent (Invitrogen). siRNAs specific for human c-Src mRNA (5′-CCACCUUUGU-GGCCCUCUATT-3′) or human MET mRNA (5′-ACAAGAUCGUCAACAAAAATT-3′) as well as a nonspecific siRNA (control) were obtained from Nippon EGT. The cells were then subjected to flow cytometry, immunoblot analysis, or assay of cell growth inhibition.

Statistical analysis. Data were analyzed by Student's two-tailed *t* test. A *P* value of <0.05 was considered statistically significant.

Results

Effects of dasatinib on the growth of gastric cancer cell lines. The baseline levels of total c-Src and activated c-Src (phospho-Y416) in 16 human gastric cancer cell lines were measured by immunoblot analysis. All the cell lines expressed detectable levels of total c-Src, whereas all lines with the exception of SNU1 and HSC39 manifested detectable (albeit different) levels of c-Src phosphorylation (Fig. 1A).

To assess the effects of dasatinib on cell growth, we exposed the gastric cancer cell lines to various concentrations of the drug and then measured cell viability. Seven cell lines were responsive to dasatinib with IC_{50} values ranging from approximately 40 to 540 nmol/L, whereas nine cell lines remained resistant to dasatinib at concentrations up to 5 μmol/L (Table 1; Fig. 1B). SNU1 and HSC39 cells, both of which seemed to lack activated c-Src, were resistant to dasatinib. For the remaining cell lines positive for phosphorylated c-Src, there was no apparent correlation between the antiproliferative effect of dasatinib and the baseline phosphorylation level of c-Src (Fig. 1A).

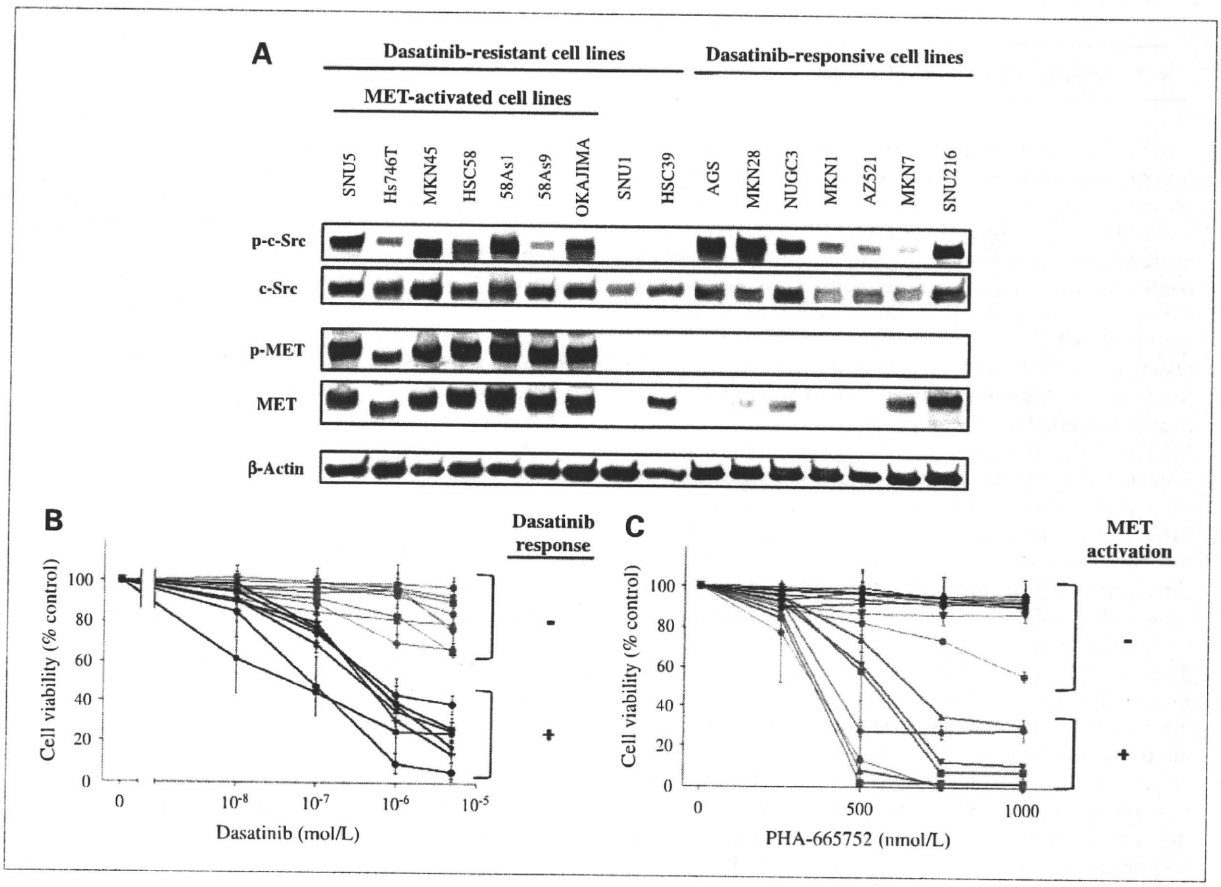

Figure 1. Phosphorylation of c-Src or MET and growth-inhibitory effects of c-Src or MET inhibitors in gastric cancer cell lines. A, the indicated gastric cancer cell lines maintained in a medium containing 10% serum were lysed and subjected to immunoblot analysis with antibodies to phosphorylated (p-) or total forms of c-Src or MET or to β-actin (loading control). B and C, gastric cancer cell lines were cultured in medium containing 10% serum for 72 hours in the presence of various concentrations of dasatinib (B) or PHA-665752 (C), after which cell viability was assessed as described in Materials and Methods. The number of viable cells is expressed as a percentage of the value for nontreated cells. Black and red lines, dasatinib-responsive and dasatinib-resistant cells, respectively. Points, mean of values from three independent experiments; bars, SD.

Table 1. IC_{50} values of dasatinib for inhibition of the growth of gastric cancer cells *in vitro*

Dasatinib response	Cell line	Dasatinib IC_{50} (μmol/L)	MET activation
Resistant	SNU5	>5	+
	Hs746T	>5	+
	MKN45	>5	+
	HSC58	>5	+
	58As1	>5	+
	58As9	>5	+
	OKAJIMA	>5	+
	SNU1	>5	
	HSC39	>5	
Responsive			
Moderately responsive	AGS	0.54 ± 0.12	
	MKN28	0.50 ± 0.11	
	NUGC3	0.45 ± 0.16	
	MKN7	0.42 ± 0.26	
	MKN1	0.28 ± 0.20	
Highly responsive	AZ521	0.06 ± 0.03	
	SNU216	0.04 ± 0.03	

NOTE: Data are means ± SD of triplicates from experiments that were repeated a total of three times with similar results.

MET activation is associated with dasatinib resistance in gastric cancer cell lines. The level of c-Src phosphorylation was thus not sufficient to distinguish dasatinib-responsive from dasatinib-resistant cells. Redundancy of tyrosine kinases has been shown to contribute to *de novo* resistance to tyrosine kinase inhibitors (21, 22). Given that amplification of *MET* is frequent in gastric cancer (23–25), we examined whether resistance to dasatinib in gastric cancer cell lines positive for c-Src activation might be due to MET activation. We first determined the abundance and activation status of MET in the gastric cancer cell lines. Immunoblot analysis revealed that all dasatinib-resistant cells positive for phosphorylated c-Src manifested high levels of both MET expression and baseline activation, as reflected by phosphorylation of tyrosine residues 1234/1235 (Fig. 1A) and tyrosine-1349 (data not shown). In contrast, cells categorized as responsive to dasatinib had undetectable levels of phosphorylated MET. We next examined the gastric cancer cell lines for *MET* amplification by fluorescence *in situ* hybridization analysis. Six of the seven cell lines positive for MET activation, all of which were resistant to dasatinib, were found to be positive for *MET* amplification, whereas the one remaining cell line (OKAJIMA) showed no evidence of *MET* amplification. In contrast, all dasatinib-responsive cell lines as well as SNU1 and HSC39 were found to be negative for *MET* amplification (data not shown). These results thus suggested that MET activation is associated with dasatinib resistance in gastric cancer cells.

A MET inhibitor suppresses the growth of dasatinib-resistant gastric cancer cell lines with activated MET but not that of dasatinib-responsive cells. The specific MET inhibitor PHA-665752 was previously shown to inhibit the proliferation of cancer cells in which MET is constitutively activated (26, 27). Given that MET was found to be activated in all dasatinib-resistant gastric cancer cell lines with activated c-Src (Fig. 1A), we examined the effect of PHA-665752 on the growth of gastric cancer cell lines. Consistent with previous observations (27), PHA-665752 inhibited the growth of the dasatinib-resistant cell lines with activated MET (Fig. 1C). In contrast, all dasatinib-responsive cell lines as well as SNU1 and HSC39 were resistant to PHA-665752 (Fig. 1C). These results thus suggested that the subsets of gastric cancer cells defined by the response to c-Src or MET inhibitors are distinct and nonoverlapping.

Dasatinib inhibits ERK or AKT signaling in dasatinib-responsive gastric cancer cell lines but not in dasatinib-resistant cells. The effects of dasatinib on cell signaling were evaluated in the gastric cancer cell lines with activated c-Src. Cells were exposed to various concentrations of dasatinib and then subjected to immunoblot analysis of phosphorylated and total forms of c-Src, ERK, and AKT (Fig. 2). Dasatinib induced marked inhibition of c-Src phosphorylation in all cell lines tested. In dasatinib-responsive cells, dasatinib also inhibited ERK phosphorylation in a concentration-dependent manner. It also inhibited AKT phosphorylation in SNU216, AGS, and MKN1 cells. In contrast, dasatinib exhibited no substantial inhibitory effect on the phosphorylation of ERK or AKT even at a concentration of 300 nmol/L in dasatinib-resistant cells. These findings indicated that the antiproliferative effect of dasatinib in gastric cancer cells correlates with the inhibition of ERK or AKT signaling.

Dasatinib induces G1 arrest or apoptosis in dasatinib-responsive gastric cancer cell lines. To investigate the mechanism by which dasatinib inhibits gastric cancer cell growth, we first analyzed the cell cycle profile by flow cytometry after exposure of cells to the drug for 0, 24, or 48 hours. We chose a dasatinib concentration of 300 nmol/L for these experiments because it approximated the IC_{50} values for dasatinib-responsive cell lines. Dasatinib increased the percentage of cells in G_0-G_1 phase of the cell cycle and decreased the percentage of those in S phase in a subset of dasatinib-responsive cell lines, including AZ521, MKN28, NUGC3, and MKN7 (Fig. 3A). The other dasatinib-responsive cell lines, including SNU216, MKN1, and AGS, in which dasatinib inhibited both ERK and AKT phosphorylation, showed an increase in the sub-G_1 cell population on exposure to dasatinib, indicative of the induction of apoptosis (Fig. 3A). In dasatinib-resistant cells with MET activation, dasatinib had minimal effects on cell cycle distribution (Supplementary Fig. S1A). We also examined the effect of dasatinib on the abundance of the cyclin-dependent kinase inhibitor p27, which contributes to the regulation of G_1-S progression. Dasatinib induced the upregulation of p27 in the four dasatinib-responsive cell lines in which it induced G_1 arrest (Fig. 3B), but not in cell lines in which it did not trigger such arrest (Supplementary Fig. S1B). As a further test for apoptosis in SNU216, MKN1, and AGS cells, we measured the activity of caspase-3 and probed for cleavage of PARP. Dasatinib increased caspase-3 activity (Fig. 3C) and induced PARP cleavage (Fig. 3D) in these three cell lines. These findings thus indicated that induction of G_1 arrest or apoptosis underlies the antiproliferative effect of dasatinib in responsive cells. On the other hand, PHA-665752 was previously shown to induce apoptosis in gastric cancer cells with *MET* amplification (27). Consistent with these previous results, we showed that PHA-665752 induced a substantial increase in the frequency of apoptosis, as revealed by an increase in caspase-3 activity and PARP cleavage, in dasatinib-resistant cells with MET activation, whereas PHA-665752 had minimal effects on apoptosis in dasatinib-responsive cells (Fig. 3C and D).

Effects of c-Src depletion in dasatinib-responsive gastric cancer cell lines. To verify that the inhibitory effect of dasatinib on cell growth is indeed mediated by c-Src inhibition rather than by nonspecific inhibition of

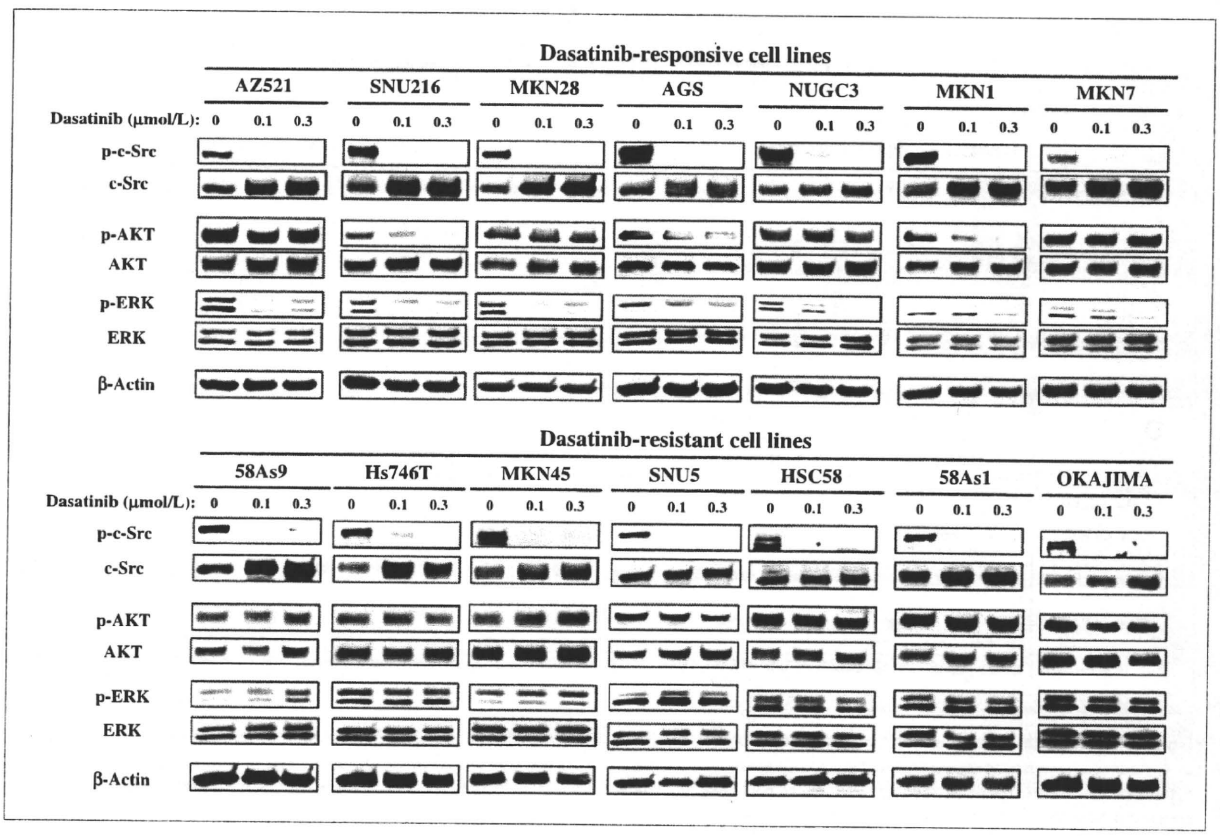

Figure 2. Effects of dasatinib on cell signaling in gastric cancer cell lines. The indicated cell lines were incubated in a medium containing 10% serum for 24 hours in the absence or presence of dasatinib at 100 or 300 nmol/L. Cell lysates were then subjected to immunoblot analysis with antibodies to the indicated proteins.

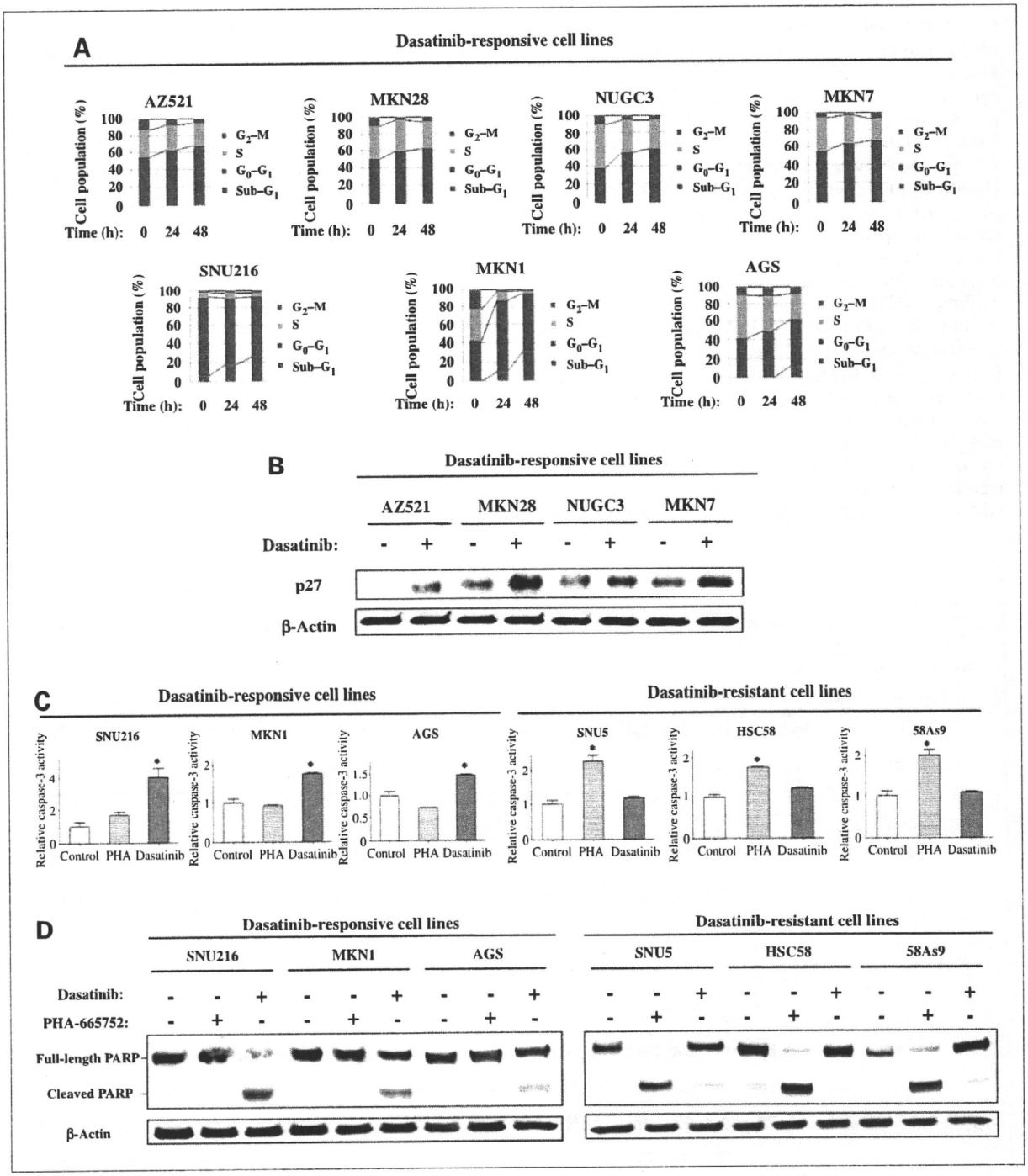

Figure 3. Effects of dasatinib on cell cycle distribution and apoptosis in gastric cancer cell lines. A, cells were incubated in medium containing 10% serum for 0, 24, or 48 hours in the presence of 300 nmol/L dasatinib, after which they were fixed, stained with propidium iodide, and analyzed for cell cycle distribution by flow cytometry. All data are means of triplicates from experiments that were repeated a total of three times with similar results. B, cells were incubated in a medium containing 10% serum for 24 hours in the absence or presence of dasatinib (300 nmol/L). Cell lysates were then subjected to immunoblot analysis with antibodies to p27. C, cells were incubated in medium containing 10% serum for 48 hours in the absence or presence of either dasatinib (300 nmol/L) or PHA-665752 (500 nmol/L). Cell lysates were then assayed for caspase-3 activity. Columns, mean of values from three independent experiments; bars, SD. *, $P < 0.05$ versus the corresponding value for control cells. D, cells were incubated in medium containing 10% serum for 72 hours in the absence or presence of either dasatinib (300 nmol/L) or PHA-665752 (500 nmol/L). Cell lysates were then subjected to immunoblot analysis with antibodies to PARP.

other kinases such as the platelet-derived growth factor receptor, c-Kit, or Bcr-Abl (6), we transfected dasatinib-responsive cells with an siRNA that targets c-Src mRNA. Similar to the effects of dasatinib, depletion of c-Src resulted in G_1 arrest (Fig. 4A), accompanied by accumulation of p27 (Fig. 4B), in AZ521, MKN28, NUGC3, or MKN7 cells. Moreover, also similar to the effects of dasatinib, depletion of c-Src in SNU216, MKN1, or AGS cells triggered apoptosis as revealed by an increase in the sub-G_1 cell population (Fig. 4A) and PARP cleavage (Fig. 4C). These results thus indicated that the effects of dasatinib on cell growth or survival in gastric cancer cell lines are mediated by inhibition of c-Src.

Mechanism of dasatinib resistance in gastric cancer cells with MET activation. Given the association of activated MET with resistance to dasatinib, we examined whether the depletion of MET might affect dasatinib cytotoxicity in dasatinib-resistant cells with MET activation. Immunoblot analysis revealed that transfection of 58As9 or OKAJIMA cells with an siRNA specific for MET mRNA resulted in the marked depletion of the corresponding protein (Fig. 5A). Such depletion of MET restored the sensitivity of these dasatinib-resistant cells to the inhibition of cell growth by dasatinib (Fig. 5B). These results thus indicated that activated MET indeed contributes to dasatinib resistance in gastric cancer cells.

To examine the mechanism by which MET activation gives rise to dasatinib resistance, we determined the effects of PHA-665752 or dasatinib on the phosphorylation of MET, c-Src, ERK, and AKT in gastric cancer cells with MET activation. PHA-665752 inhibited the phosphorylation of MET, c-Src, AKT, and ERK in such cells (Fig. 5C). In contrast, dasatinib had no effect on either MET phosphorylation or downstream signaling by AKT or ERK in these cells (Fig. 5D). These data thus suggested that MET activation results in AKT and ERK phosphorylation in a c-Src–independent manner, although c-Src is activated at least in part by increased MET signaling in dasatinib-resistant cells with MET activation.

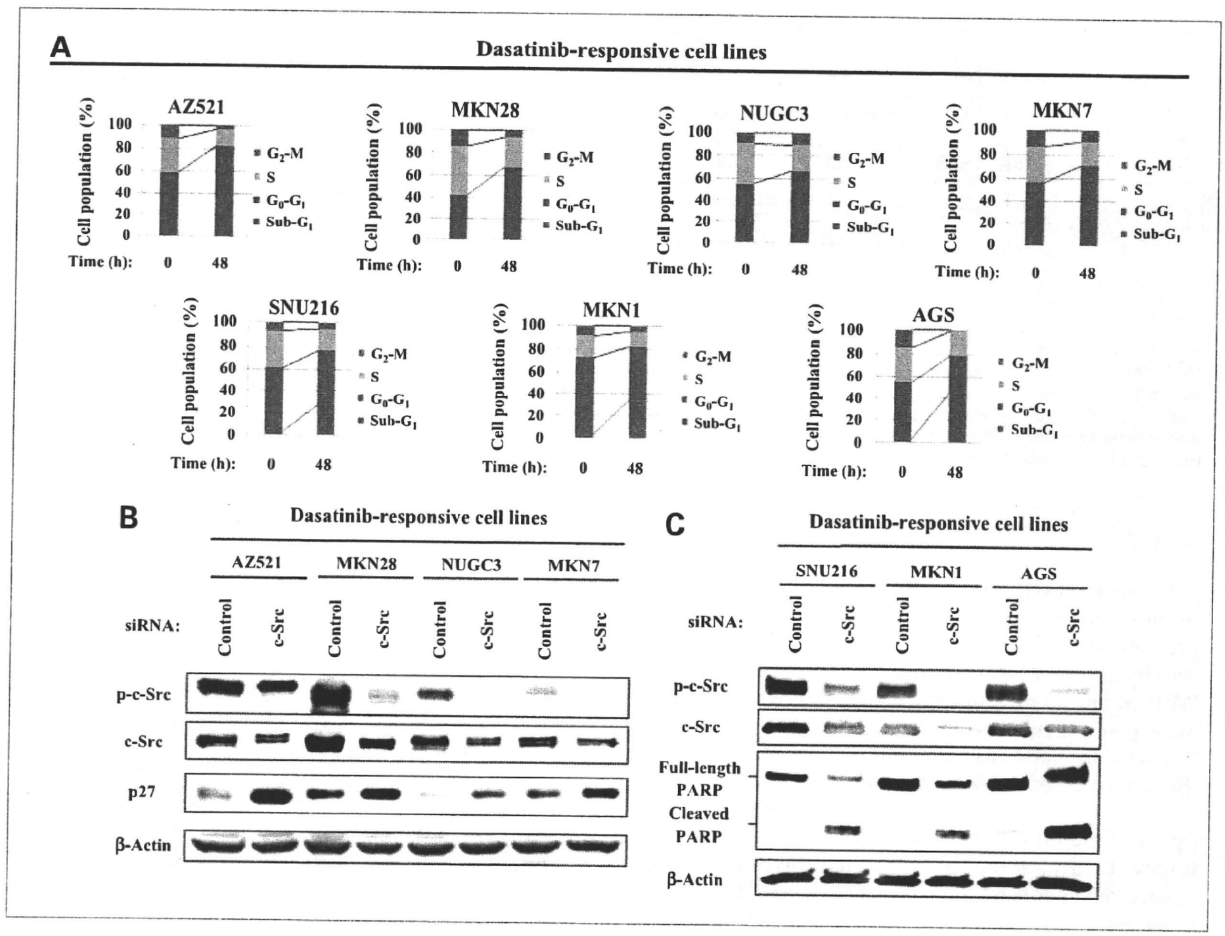

Figure 4. Effects of c-Src depletion on cell cycle distribution and apoptosis in gastric cancer cell lines. A, cells were transfected with nonspecific (control) or c-Src siRNAs for 48 hours, fixed, stained with propidium iodide, and analyzed for cell cycle distribution by flow cytometry. All data are means of triplicates from experiments that were repeated a total of three times with similar results. B and C, cells were transfected as in A for 48 hours (B) or 72 hours (C), after which cell lysates were subjected to immunoblot analysis with antibodies to the indicated proteins.

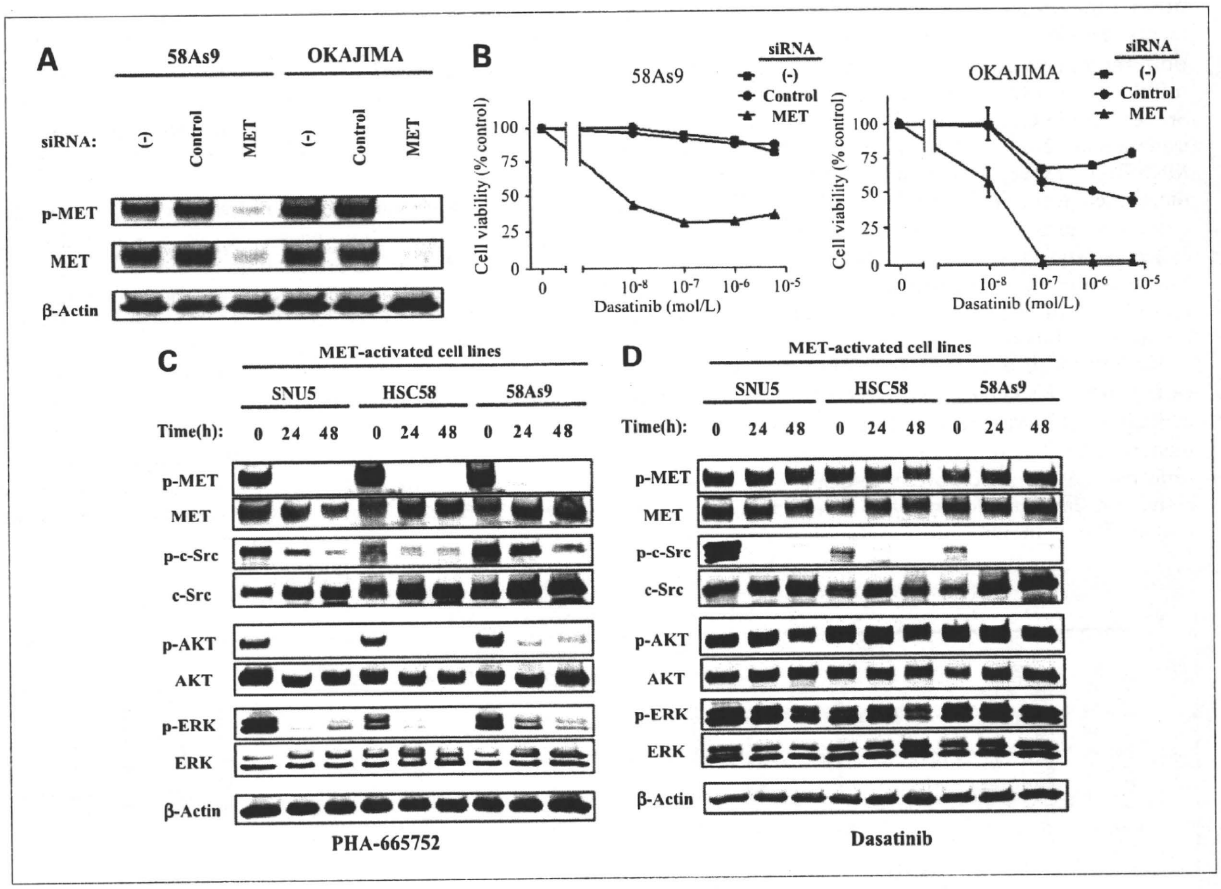

Figure 5. Mechanism of dasatinib resistance in gastric cancer cells with MET activation. A, cells were transfected or not with nonspecific (control) or MET siRNAs for 48 hours, after which cell lysates were subjected to immunoblot analysis with antibodies to the indicated proteins. B, cells transfected as in A were cultured in a medium containing 10% serum and various concentrations of dasatinib for an additional 48 hours, after which cell viability was assessed. The number of viable cells is expressed as a percentage of the corresponding value for cells not exposed to dasatnib. Points, mean of values from three independent experiments; bars, SD. C and D, cells were incubated in medium containing 10% serum for 0, 24, or 48 hours in the presence of 500 nmol/L PHA-665752 (C) or 300 nmol/L dasatinib (D). Cell lysates were then subjected to immunoblot analysis with antibodies to the indicated proteins.

Discussion

We have shown that c-Src is activated at various levels in most human gastric cancer cell lines, consistent with previous studies showing the upregulation of the kinase activity of c-Src in most gastric cancers examined (15–18). We therefore investigated the potential utility of c-Src as a molecular target for treatment of gastric cancer. Dasatinib has been developed as a multikinase inhibitor with activity against c-Src, Bcr-Abl, and several receptor tyrosine kinases (6). We examined the effects of c-Src inhibition by dasatinib on cell growth in gastric cancer cell lines, finding that dasatinib inhibited the growth of a subset of such cell lines exhibiting c-Src phosphorylation. No relation was apparent between the response to dasatinib and the level of c-Src phosphorylation in cell lines with activated c-Src, whereas SNU1 and HSC39, both of which did not manifest detectable c-Src phosphorylation, were resistant to dasatinib, consistent with previous observations (7, 8, 14, 28, 29). These findings suggest that c-Src promotes cell proliferation and survival in a subset of gastric cancer cell lines positive for c-Src activation but not in those without c-Src activation.

We found that the level of ERK phosphorylation was reduced by dasatinib in all responsive cell lines but not in resistant cell lines, suggesting that the inhibition of ERK might correlate with the antiproliferative effects of c-Src inhibitors in gastric cancer cells. In addition, inhibition of both ERK and AKT phosphorylation by dasatinib was associated with the induction of apoptosis in SNU216, MKN1, and AGS cells. To confirm that the effects of dasatinib on cell cycle progression and apoptosis are indeed attributable to c-Src inhibition in dasatinib-responsive gastric cancer cells, we specifically depleted the cells of c-Src by RNA interference. In cells in which dasatinib induced G_1 arrest, depletion of c-Src also triggered G_1 arrest accompanied by the upregulation of p27. Similarly, in cells in which dasatinib induced apoptosis, c-Src depletion also

elicited apoptosis, as revealed by the detection of PARP cleavage. These data thus provide more definitive support for the notion that c-Src signaling promotes the proliferation and survival of dasatinib-responsive gastric cancer cell lines. A c-Src inhibitor was previously shown to induce G_1 arrest in prostate cancer cells (11). On the other hand, dasatinib was found to induce apoptosis in non–small cell lung cancer cells harboring an epidermal growth factor receptor gene mutation (8). Sensitive cells thus exhibit different responses to c-Src inhibitors. The mechanisms underlying the cellular decision to undergo G_1 arrest or apoptosis in response to such inhibitors remain unclear but may be related to differences in cell type.

Gastric cancer cell lines positive for MET activation were resistant to dasatinib, despite the activation of c-Src apparent in these cells. We showed that dasatinib sensitivity was restored in such cells by the depletion of MET, suggesting that MET activation contributes to resistance to c-Src inhibitors. The MET inhibitor PHA-665752 suppressed c-Src, ERK, and AKT phosphorylation in cells with activated MET, whereas dasatinib had minimal effects on either ERK or AKT phosphorylation. These findings suggested that MET-c-Src and MET-ERK/AKT pathways operate independently of each other in such cells. We found that PHA-665752 inhibited the growth of cells with MET activation, with this effect being accompanied by the induction of apoptosis. Consistent with our findings, *MET* amplification was previously shown to identify a subset of gastric cancers likely to respond to MET inhibitors (27). These results suggest that cells with MET activation may have switched their cell growth dependence from the c-Src-ERK/AKT pathway to the MET-ERK/AKT pathway, although the precise mechanism of the altered signal transduction remains unknown. We further found that the combination of dasatinib and PHA-665752 manifested an additive to synergistic inhibitory effect on the growth of gastric cancer cells with MET activation but not on that of cells without MET activation (Supplementary Table S1 and Fig. S2). These data suggest that the survival of cells with MET activation depends at least in part on activated c-Src in the presence of a MET inhibitor. Further studies are required to determine the mechanism of dasatinib resistance in gastric cancer with MET activation. Amplification of *MET* is often responsible for the activation of MET signaling, with such amplification occurring most frequently (10-20%) in gastric cancer (23–25). Our data therefore suggest that the analysis of *MET* amplification might optimize patient selection for gastric cancer treatment with c-Src or MET inhibitors.

The recent success of molecularly targeted agents seems to depend on the identification of drug targets and patients who are likely to benefit from these agents. In the present study, we show that c-Src is a promising target for the treatment of gastric cancer. Moreover, our results indicate that testing to exclude the possibility of *MET* amplification should be done in consideration of c-Src inhibitors for the treatment of gastric cancer. Dasatinib inhibited the growth of SNU216 and AZ521 cells with IC_{50} values in the low nanomolar range (40 and 60 nmol/L, respectively); however, the IC_{50} values for most of the responsive cell lines were greater than the maximum achievable plasma concentration (100 nmol/L) of dasatinib (30, 31). Novel c-Src inhibitors with increased potency are currently under development (32) and might prove beneficial for the treatment of gastric cancer. Our results provide a rationale for future clinical investigation of the therapeutic efficacy of c-Src inhibitors in individuals with gastric cancer as well as for the selection of patients likely to benefit from such treatment.

Disclosure of Potential Conflicts of Interest

No potential conflicts of interest were disclosed.

Acknowledgments

The costs of publication of this article were defrayed in part by the payment of page charges. This article must therefore be hereby marked *advertisement* in accordance with 18 U.S.C. Section 1734 solely to indicate this fact.

Received 01/04/2010; revised 02/22/2010; accepted 03/03/2010; published OnlineFirst 04/20/2010.

References

1. Hartgrink HH, Jansen EP, van Grieken NC, van de Velde CJ. Gastric cancer. Lancet 2009;374:477–90.
2. Wesolowski R, Lee C, Kim R. Is there a role for second-line chemotherapy in advanced gastric cancer? Lancet Oncol 2009;10:903–12.
3. Kim LC, Song L, Haura EB. Src kinases as therapeutic targets for cancer. Nat Rev Clin Oncol 2009;6:587–95.
4. Yeatman TJ. A renaissance for SRC. Nat Rev Cancer 2004;4:470–80.
5. Irby RB, Yeatman TJ. Role of Src expression and activation in human cancer. Oncogene 2000;19:5636–42.
6. Lombardo LJ, Lee FY, Chen P, et al. Discovery of N-(2-chloro-6-methyl-phenyl)-2-(6-(4-(2-hydroxyethyl)-piperazin-1-yl)-2-methylpyrimidin-4-ylamino)thiazole-5-carboxamide (BMS-354825), a dual Src/Abl kinase inhibitor with potent antitumor activity in preclinical assays. J Med Chem 2004;47:6658–61.
7. Johnson FM, Saigal B, Talpaz M, Donato NJ. Dasatinib (BMS-354825) tyrosine kinase inhibitor suppresses invasion and induces cell cycle arrest and apoptosis of head and neck squamous cell carcinoma and non-small cell lung cancer cells. Clin Cancer Res 2005;11:6924–32.
8. Song L, Morris M, Bagui T, Lee FY, Jove R, Haura EB. Dasatinib (BMS-354825) selectively induces apoptosis in lung cancer cells dependent on epidermal growth factor receptor signaling for survival. Cancer Res 2006;66:5542–8.
9. Jallal H, Valentino ML, Chen G, Boschelli F, Ali S, Rabbani SA. A Src/Abl kinase inhibitor, SKI-606, blocks breast cancer invasion, growth, and metastasis *in vitro* and *in vivo*. Cancer Res 2007;67:1580–8.
10. Zhang J, Kalyankrishna S, Wislez M, et al. SRC-family kinases are activated in non-small cell lung cancer and promote the survival of epidermal growth factor receptor-dependent cell lines. Am J Pathol 2007;170:366–76.
11. Chang YM, Bai L, Liu S, Yang JC, Kung HJ, Evans CP. Src family kinase oncogenic potential and pathways in prostate cancer as revealed by AZD0530. Oncogene 2008;27:6365–75.
12. Park SI, Zhang J, Phillips KA, et al. Targeting SRC family kinases

inhibits growth and lymph node metastases of prostate cancer in an orthotopic nude mouse model. Cancer Res 2008;68:3323–33.
13. Leung EL, Tam IY, Tin VP, et al. SRC promotes survival and invasion of lung cancers with epidermal growth factor receptor abnormalities and is a potential candidate for molecular-targeted therapy. Mol Cancer Res 2009;7:923–32.
14. Nautiyal J, Majumder P, Patel BB, Lee FY, Majumdar AP. Src inhibitor dasatinib inhibits growth of breast cancer cells by modulating EGFR signaling. Cancer Lett 2009;283:143–51.
15. Takekura N, Yasui W, Yoshida K, et al. pp60c-src protein kinase activity in human gastric carcinomas. Int J Cancer 1990;45:847–51.
16. Masaki T, Shiratori Y, Okada H, et al. pp60c-src activation in gastric carcinoma: a preliminary study. Am J Gastroenterol 2000;95:837–8.
17. Humar B, Fukuzawa R, Blair V, et al. Destabilized adhesion in the gastric proliferative zone and c-Src kinase activation mark the development of early diffuse gastric cancer. Cancer Res 2007;67:2480–9.
18. Peng L, Ran YL, Hu H, et al. Secreted LOXL2 is a novel therapeutic target that promotes gastric cancer metastasis via the Src/FAK pathway. Carcinogenesis 2009;30:1660–9.
19. Yanagihara K, Takigahira M, Tanaka H, et al. Development and biological analysis of peritoneal metastasis mouse models for human scirrhous stomach cancer. Cancer Sci 2005;96:323–32.
20. Wolff AC, Hammond ME, Schwartz JN, et al. American Society of Clinical Oncology/College of American Pathologists guideline recommendations for human epidermal growth factor receptor 2 testing in breast cancer. J Clin Oncol 2007;25:118–45.
21. Shattuck DL, Miller JK, Carraway KL III, Sweeney C. Met receptor contributes to trastuzumab resistance of Her2-overexpressing breast cancer cells. Cancer Res 2008;68:1471–7.
22. Lu Y, Zi X, Zhao Y, Mascarenhas D, Pollak M. Insulin-like growth factor-I receptor signaling and resistance to trastuzumab (Herceptin). J Natl Cancer Inst 2001;93:1852–7.
23. Kuniyasu H, Yasui W, Kitadai Y, Yokozaki H, Ito H, Tahara E. Frequent amplification of the c-met gene in scirrhous type stomach cancer. Biochem Biophys Res Commun 1992;189:227–32.
24. Nessling M, Solinas-Toldo S, Wilgenbus KK, Borchard F, Lichter P. Mapping of chromosomal imbalances in gastric adenocarcinoma revealed amplified protooncogenes MYCN, MET, WNT2, and ERBB2. Genes Chromosomes Cancer 1998;23:307–16.
25. Sakakura C, Mori T, Sakabe T, et al. Gains, losses, and amplifications of genomic materials in primary gastric cancers analyzed by comparative genomic hybridization. Genes Chromosomes Cancer 1999;24:299–305.
26. Christensen JG, Schreck R, Burrows J, et al. A selective small molecule inhibitor of c-Met kinase inhibits c-Met-dependent phenotypes *in vitro* and exhibits cytoreductive antitumor activity *in vivo*. Cancer Res 2003;63:7345–55.
27. Smolen GA, Sordella R, Muir B, et al. Amplification of MET may identify a subset of cancers with extreme sensitivity to the selective tyrosine kinase inhibitor PHA-665752. Proc Natl Acad Sci U S A 2006;103:2316–21.
28. Zhang Q, Thomas SM, Xi S, et al. SRC family kinases mediate epidermal growth factor receptor ligand cleavage, proliferation, and invasion of head and neck cancer cells. Cancer Res 2004;64:6166–73.
29. Shor AC, Keschman EA, Lee FY, et al. Dasatinib inhibits migration and invasion in diverse human sarcoma cell lines and induces apoptosis in bone sarcoma cells dependent on SRC kinase for survival. Cancer Res 2007;67:2800–8.
30. Christopher LJ, Cui D, Wu C, et al. Metabolism and disposition of dasatinib after oral administration to humans. Drug Metab Dispos 2008;36:1357–64.
31. Kim DW, Goh YT, Hsiao HH, et al. Clinical profile of dasatinib in Asian and non-Asian patients with chronic myeloid leukemia. Int J Hematol 2009;89:664–72.
32. Lau GM, Yu GL, Gelman IH, Gutowski A, Hangauer D, Fang JW. Expression of Src and FAK in hepatocellular carcinoma and the effect of Src inhibitors on hepatocellular carcinoma *in vitro*. Dig Dis Sci 2009;54:1465–74.

British Journal of Cancer (2010) 103, 354–361

www.bjcancer.com

Identification of thymidylate synthase as a potential therapeutic target for lung cancer

K Takezawa[1], I Okamoto*[,1], S Tsukioka[2], J Uchida[2], M Kiniwa[2], M Fukuoka[3] and K Nakagawa[1]

[1]Department of Medical Oncology, Kinki University School of Medicine, 377-2 Ohno-higashi, Osaka-Sayama, Osaka 589-8511, Japan; [2]Tokushima Research Center, Taiho Pharmaceutical Co. Ltd, 224-2 Hiraishi-ebisuno, Kawauchi, Tokushima 771-0194, Japan; [3]Department of Medical Oncology, Kinki University School of Medicine, Sakai Hospital, 2-7-1 Harayamadai, Minami-ku Sakai, Osaka 590-0132, Japan

BACKGROUND: Thymidylate synthase (TS), a key enzyme in the *de novo* synthesis of thymidine, is an important chemotherapeutic target for malignant tumours including lung cancer. Although inhibition of TS has an antiproliferative effect in cancer cells, the precise mechanism of this effect has remained unclear.

METHODS: We examined the effects of TS inhibition with an RNA interference-based approach. The effect of TS depletion on the growth of lung cancer cells was examined using colorimetric assay and flow cytometry.

RESULTS: Measurement of the enzymatic activity of TS in 30 human lung cancer cell lines revealed that such activity differs among tumour histotypes. Almost complete elimination of TS activity by RNA interference resulted in inhibition of cell proliferation in all tested cell lines, suggestive of a pivotal role for TS in cell proliferation independent of the original level of enzyme activity. The antiproliferative effect of TS depletion was accompanied by arrest of cells in S phase of the cell cycle and the induction of caspase-dependent apoptosis as well as by changes in the expression levels of cyclin E and c-Myc. Moreover, TS depletion induced downregulation of the antiapoptotic protein X-linked inhibitor of apoptosis (XIAP), and it seemed to activate the mitochondrial pathway of apoptosis.

CONCLUSION: Our data provide insight into the biological relevance of TS as well as a basis for clinical development of TS-targeted therapy for lung cancer.

British Journal of Cancer (2010) **103,** 354–361. doi:10.1038/sj.bjc.6605793 www.bjcancer.com
Published online 13 July 2010

Keywords: thymidylate synthase; lung cancer; RNA interference; apoptosis; cell cycle

Translational Therapeutics

Thymidylate synthase (TS) is an essential enzyme that catalyses the transfer of a methyl group from methylenetetrahydrofolate to dUMP to generate dTMP (Carreras and Santi, 1995). The subsequent phosphorylation of dTMP to dTTP provides a direct precursor for DNA synthesis. The level of TS expression is increased in highly proliferative cells, and an increased abundance of TS in a broad range of tumours is associated with a poor treatment response and prognosis (Costi *et al*, 2005). Transfection of nontransformed cells with an expression vector for TS has also been found to confer transformed-like behaviour, suggesting that TS itself is a potential oncoprotein (Rahman *et al*, 2004). These findings have led to TS being considered as a molecular target for cancer therapy. To date, the antiproliferative effect of TS inhibition has been examined mostly with the use of drugs such as 5-fluorouracil and its active metabolite 5-fluoro-dUMP, the former of which is used in cancer chemotherapy. Although studies with antisense oligodeoxynucleotides have also shown that depletion of TS results in growth inhibition in human tumour cells (Ferguson *et al*, 1999; Lin *et al*, 2001; Flynn *et al*, 2006), the underlying mechanism of the antiproliferative effect of specific TS inhibition has remained largely unknown.

*Correspondence: Dr I Okamoto;
E-mail: chi-okamoto@dotd.med.kindai.ac.jp
Received 8 June 2010; revised 17 June 2010; accepted 24 June 2010; published online 13 July 2010

Lung cancer is one of the most common forms of cancer worldwide. Advanced lung cancer is treated by combination chemotherapy, although further improvement in such therapy is warranted. High levels of TS in tumours have been associated with a poor response to TS-targeting agents in individuals with advanced lung cancer (Oguri *et al*, 2005; Kubota *et al*, 2009; Ozasa *et al*, 2009), although the biological relevance of TS in lung cancer has remained to be well established. We have now abrogated both the expression and activity of TS in lung cancer cells by the application of RNA interference (RNAi). With this approach, we investigated the precise mechanism of the antiproliferative effect of TS depletion in lung cancer cells and further examined the potential role of TS as a target for chemotherapeutic agents in these cells. Our results provide a basis for the further development of TS-targeted therapy in lung cancer patients.

MATERIALS AND METHODS

Cell culture and reagents

The human lung cancer cell lines A549, H1975, H1650, H358, SW1573, H460, H1299, H520, Calu-1, H226, H82, H526, and H69 were obtained from American Type Culture Collection (Manassas, VA, USA); PC9 and PC9/ZD were obtained as described previously (Koizumi *et al*, 2005); PC3, LK2, PC1, EBC-1, PC10, HARA, SBC-3,

MS-1, COR-L47, STC-1, SBC-1, and RERF-LC-MA were obtained from Human Science Research Resources Bank (Osaka, Japan); Lu135 and Lu134B were from Riken Cell Bank (Tokyo, Japan); and QG56 was obtained from Immuno-Biological Laboratories (Gunma, Japan). All cells were cultured under a humidified atmosphere of 5% CO_2 at 37°C in RPMI 1640 medium (Sigma, St Louis, MO, USA) supplemented with 10% fetal bovine serum. The pan-caspase inhibitor ZVAD-FMK was from Wako (Osaka, Japan).

Assay of TS activity

Thymidylate synthase activity was quantified using tritiated 5-fluoro-dUMP binding assay (Spears *et al*, 1984). Cells were harvested, diluted in 0.2 M Tris-HCl (pH 7.4) containing 20 mM 2-mercaptoethanol, 15 mM CMP, and 100 mM NaF, and disrupted by ultrasonic treatment. The cell lysate was centrifuged at 1600 g for 15 min at 4°C, and the resulting supernatant was centrifuged at 105 000 g for 1 h at 4°C. A portion (50 μl) of the final supernatant was mixed consecutively with 50 μl of Buffer A (600 mM NH_4HCO_3 buffer (pH 8.0), 100 mM 2-mercaptoethanol, 100 mM NaF, and 15 mM CMP) and with 50 μl of [6-^{3}H]5-fluoro-dUMP (7.8 pmol) plus 25 μl of cofactor solution (50 mM potassium phosphate buffer (pH 7.4), 20 mM 2-mercaptoethanol, 100 mM NaF, 15 mM CMP, 2% bovine serum albumin, 2 mM tetrahydrofolic acid, 16 mM sodium ascorbate, and 9 mM formaldehyde). The resulting mixture was incubated at 30°C for 20 min, after which the reaction was terminated by the addition of 100 μl of 2% bovine serum albumin and 275 μl of 1 M $HClO_4$ and by centrifugation at 1630 g for 15 min at 4°C. The resulting precipitate was suspended in 2 ml of 0.5 M $HClO_4$, and the mixture was subjected to ultrasonic treatment followed by centrifugation at 1600 g for 15 min at 4°C. The final precipitate was solubilised with 0.5 ml of 98% formic acid, mixed with 10 ml of ACS II scintillation fluid, and assayed for radioactivity.

RNAi

Cells were plated at 50–60% confluence in six-well plates or 25 cm^2 flasks and then incubated for 24 h before transient transfection for the indicated times with small interfering RNAs (siRNAs) mixed with the Lipofectamine reagent (Invitrogen, Carlsbad, CA, USA). The siRNAs specific for TS mRNA (TS-1, 5′-CAAUCCGCAUCCA ACUAUU-3′; TS-2, 5′-GCUCAGGAUUCUUCGAAAA-3′; and TS-3, 5′-AGCUCAGGAUUCUUCGAAA-3′) and a nonspecific siRNA (5′-GUUGAGAGAUAUUAGAGUU-3′) were obtained from Nippon EGT (Toyama, Japan). The cells were then subjected to immunoblot analysis, flow cytometry, or assay of TS or caspase-3 activity.

Immunoblot analysis

Cells were washed twice with ice-cold phosphate-buffered saline (PBS) and then lysed in a solution containing 20 mM Tris-HCl (pH 7.5), 150 mM NaCl, 1 mM EDTA, 1% Triton X-100, 2.5 mM sodium pyrophosphate, 1 mM phenylmethylsulfonyl fluoride, and leupeptin (1 μg ml^{-1}). The protein concentration of cell lysates was determined using the Bradford reagent (Bio-Rad, Hercules, CA, USA), and equal amounts of protein were subjected to SDS–polyacrylamide gel electrophoresis on a 7.5 or 12% gel. The separated proteins were transferred to a nitrocellulose membrane, which was then exposed to 5% nonfat dried milk in PBS for 1 h at room temperature before incubation overnight at 4°C either with rabbit polyclonal antibodies to TS (1 : 1000 dilution; Santa Cruz Biotechnology, Santa Cruz, CA, USA), β-actin (1 : 500 dilution, Sigma), survivin (1 : 1000 dilution; R&D Systems, Minneapolis, MN, USA), or c-Myc, poly(ADP-ribose) polymerase (PARP), Bcl-2, Bcl-x_L, Bax, Bak, X-linked inhibitor of apoptosis (XIAP), or Omi/HtrA2 (all in a 1 : 1000 dilution and from Cell Signaling Technology, Danvers, MA, USA) or with mouse monoclonal antibodies to cyclin E (1 : 1000 dilution, Santa Cruz Biotechnology), cytochrome *c* (1 : 1000 dilution, Cell Signaling Technology), to Smac/Diablo (1 : 1000 dilution, Cell Signaling Technology). The membrane was then washed with PBS containing 0.05% Tween 20 before incubation for 1 h at room temperature with horseradish peroxidase-conjugated goat antibodies to rabbit (Sigma) or mouse (Santa Cruz Biotechnology) immunoglobulin G. Immune complexes were finally detected with chemiluminescence reagents (GE Healthcare, Little Chalfont, UK).

Growth inhibition assay *in vitro* (MTT assay)

Cells were plated at 50–60% confluence in 25 cm^2 flasks and then incubated for 24 h before transient transfection with an siRNA specific for TS mRNA or a control siRNA as described above. The cells were then isolated by exposure to trypsin, transferred to 96-well flat-bottom plates, and cultured for 72 h before the addition of TetraColor One (5 mM tetrazolium monosodium salt and 0.2 mM 1-methoxy-5-methyl phenazinium methylsulfate; Seikagaku, Tokyo, Japan) to each well and incubation for an additional 3 h at 37°C. The absorbance at 490 nm of each well was measured using Multiskan Spectrum instrument (Thermo Labsystems, Boston, MA, USA), and absorbance values were expressed as a percentage of that for nontransfected control cells.

Cell cycle analysis

Cells were harvested, washed with PBS, fixed with 70% methanol, washed again with PBS, and stained with propidium iodide (0.05 mg ml^{-1}) in a solution containing 0.1% Triton X-100, 0.1 mM EDTA, and RNase A (0.05 mg ml^{-1}). The stained cells ($\sim 1 \times 10^6$) were then analysed for DNA content using flow cytometer (FACS Caliber; Becton Dickinson, Franklin Lakes, NJ, USA) and Modfit software (Verity Software House, Topsham, ME, USA).

Assay of caspase-3 activity

The activity of caspase-3 in cell lysates was measured using CCP32/Caspase-3 Fluometric Protease Assay kit (MBL, Woburn, MA, USA). Fluorescence attributable to cleavage of the Asp-Glu-Val-Asp-7-amino-4-trifluoromethyl coumarin (DEVD-AFC) substrate was measured at excitation and emission wavelengths of 390 and 460 nm, respectively.

Subcellular fractionation

A cytosolic fraction was isolated from cells by centrifugation. In brief, cells were washed, resuspended in homogenisation buffer (0.25 M sucrose, 10 mM HEPES-NaOH (pH 7.4), and 1 mM EGTA), and homogenised by 50 strokes in a Dounce homogeniser. The homogenate was centrifuged at 1000 g for 15 min at 4°C to remove nuclei and intact cells, and the resulting supernatant was centrifuged at 10 000 g for 15 min at 4°C. The final supernatant (cytosolic fraction) was subjected to immunoblot analysis.

Statistical analysis

Data were analysed using Student's two-tailed *t*-test. A *P*-value of <0.05 was considered statistically significant.

RESULTS

TS activity varies among histotypes of lung cancer cells

We first examined the enzymatic activity of TS in 30 human lung cancer cell lines (Table 1). The median TS activity in small cell lung cancer (SCLC) lines was significantly higher than that in non-SCLC (NSCLC) lines. Among NSCLC cell lines, the values for squamous cell carcinoma were higher than those for non-squamous cell

Table 1 TS activity of lung cancer cell lines classified according to histology

Cell line	Histology	TS activity (pmol per mg protein)
A549	Adeno	1.003 ± 0.142
H1975	Adeno	1.005 ± 0.276
H1650	Adeno	0.705 ± 0.177
PC9	Adeno	0.370 ± 0.042
PC9/ZD	Adeno	0.635 ± 0.148
H358	Adeno	1.140 ± 0.127
PC3	Adeno	0.591 ± 0.325
SW1573	Adeno	1.695 ± 0.544
H460	Large cell	0.420 ± 0.184
H1299	Large cell	1.121 ± 0.594
H520	Squamous	1.755 ± 0.813
Calu-1	Squamous	4.805 ± 3.061
H226	Squamous	1.930 ± 0.820
LK2	Squamous	1.121 ± 0.042
PC1	Squamous	3.055 ± 0.997
EBC-1	Squamous	1.055 ± 0.078
PC10	Squamous	1.204 ± 0.052
QG56	Squamous	0.870 ± 0.030
HARA	Squamous	2.590 ± 0.340
SBC-3	SCLC	5.795 ± 0.247
H82	SCLC	5.170 ± 0.641
H526	SCLC	1.125 ± 0.092
H69	SCLC	4.005 ± 0.078
MS-1	SCLC	2.555 ± 0.474
COR-L47	SCLC	3.760 ± 0.560
STC-1	SCLC	6.832 ± 0.490
SBC-1	SCLC	0.753 ± 0.023
Lu135	SCLC	3.698 ± 0.190
Lu134B	SCLC	0.310 ± 0.100
RERF-LC-MA	SCLC	1.413 ± 0.183

Abbreviations: SCLC = small cell lung cancer; TS = thymidylate synthase. Data are means ± s.d. from three independent experiments.

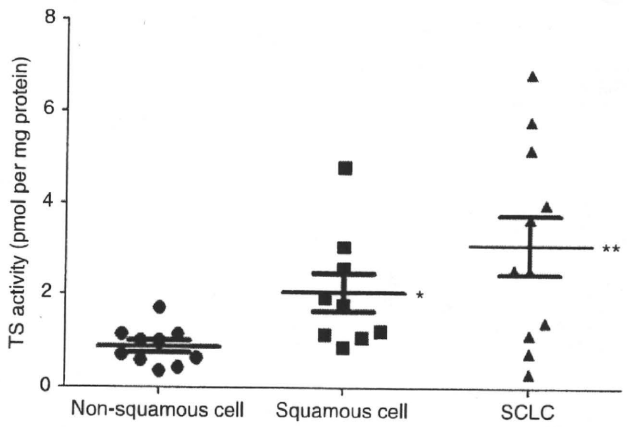

Figure 1 Thymidylate synthase (TS) activity in lung cancer cell lines stratified according to histotype. Central horizontal lines represent median values, with the upper and lower bars representing the 95% confidence interval. *$P<0.05$ for squamous cell carcinoma *vs* non-squamous cell carcinoma; **$P<0.05$ for SCLC *vs* either squamous cell or non-squamous cell carcinoma.

carcinoma (Figure 1). There was no significant correlation between TS activity and cell proliferation rate among these lung cancer cell lines (data not shown). These data thus suggested that TS activity varies according to histotype among lung cancer cell lines.

TS depletion induces growth inhibition regardless of original TS activity level in lung cancer cells

We next examined the effect of TS depletion by RNAi on the growth of lung cancer cell lines. The abundance of TS was markedly decreased as a result of cell transfection with either of three different siRNAs targeted to TS mRNA (Figure 2A). Given that the TS-1 siRNA induced the most pronounced downregulation of TS expression, we selected this siRNA for use in subsequent experiments. In all tested lung cancer cells, transfection with TS-1 resulted in marked depletion of TS, whereas no such effect was observed in cells transfected with a nonspecific siRNA (Figure 2B). Moreover, transfection of cells with TS-1 resulted in a >90% decrease in TS activity compared with that in corresponding cells transfected with a nonspecific siRNA or in untreated cells (Figure 2C), regardless of the original levels of TS expression and activity. The antiproliferative effect of TS depletion was evaluated using the MTT assay. Depletion of TS resulted in pronounced inhibition of proliferation in all tested cells compared with the corresponding cells transfected with a nonspecific siRNA or untreated cells (Figure 2D), and this antiproliferative effect was found to be time dependent (Figure 2E). These data thus suggested that the almost complete elimination of TS activity resulted in marked inhibition of the proliferation of lung cancer cells regardless of the original level of such activity.

TS depletion induces S-phase arrest in lung cancer cells

To investigate the mechanism by which TS depletion inhibits lung cancer cell growth, we examined the cell cycle profile by flow cytometry. Transfection with TS-1 siRNA increased the proportion of cells in S phase of the cell cycle and reduced that of cells in G_1 or G_2-M phases in all tested cell lines regardless of histotype (Figure 3A). Immunoblot analysis of proteins implicated in regulation of the G_1-S transition revealed that TS depletion increased the abundance of cyclin E in all tested cell lines (Figure 3B) without affecting that of cyclins D or A (data not shown). In addition, TS depletion induced downregulation of c-Myc (Figure 3B), a transcription factor that activates the expression of several cell cycle-related genes. However, expression of c-Myc was not detected in H69 cells, consistent with previous observations (Plummer *et al*, 1993). These results thus suggested that the S-phase arrest induced by TS depletion in lung cancer cells was related to upregulation of cyclin E and downregulation of c-Myc.

TS depletion induces caspase-dependent apoptosis in lung cancer cells

We next examined the effect of TS depletion on apoptosis in lung cancer cells. Flow cytometric analysis revealed that TS depletion induced a time-dependent increase in the size of the sub-G_1 (apoptotic) cell population (Figure 4A). Depletion of TS also induced the cleavage of PARP (Figure 4B), a characteristic of apoptosis, in the cell lines examined. Furthermore, the activity of caspase-3 in cell lysates was increased as a consequence of TS depletion (Figure 4C), and previous exposure of lung cancer cells to the pan-caspase inhibitor ZVAD-FMK significantly inhibited the increase in the size of the sub-G_1 cell population induced by depletion of TS (Figure 4D). These data thus indicated that TS depletion induces caspase-dependent apoptosis in lung cancer cells.

TS depletion activates the mitochondrial pathway of apoptosis and induces downregulation of XIAP

To elucidate further the mechanism of apoptosis induced by TS depletion, we examined the expression of members of the Bcl-2

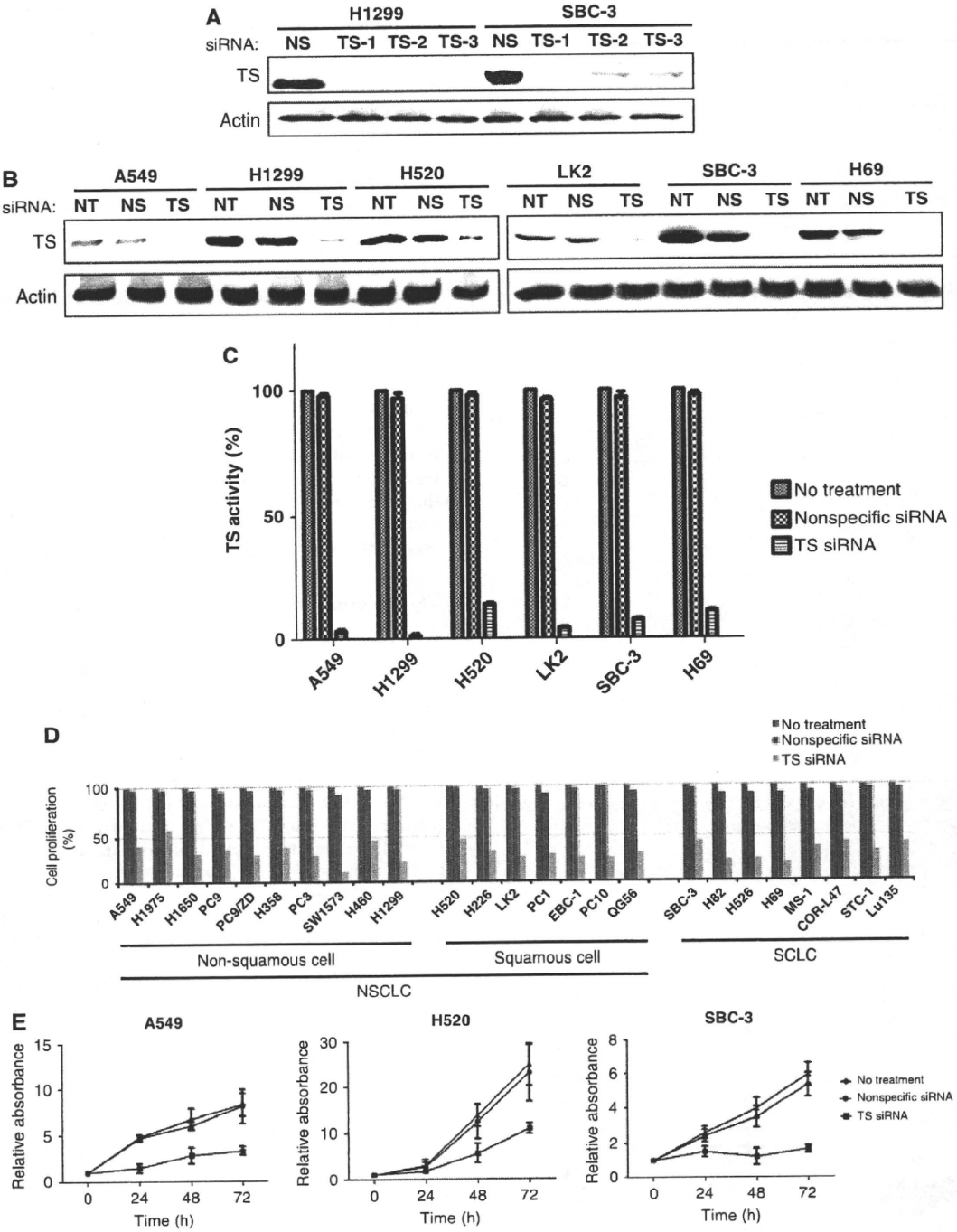

Figure 2 Effects of transient depletion of TS on TS activity and the proliferation of lung cancer cell lines. (**A**) The indicated cell lines were transfected with a nonspecific (NS) siRNA or with either of three different siRNAs specific for TS mRNA (TS-1, TS-2, and TS-3) for 48 h, after which cell lysates were prepared and subjected to immunoblot analysis with antibodies to TS and β-actin (loading control). (**B**) The indicated cell lines were left untreated (NT) or were transfected with nonspecific or TS-1 siRNAs for 48 h, after which cell lysates were prepared and subjected to immunoblot analysis with antibodies to TS and β-actin. (**C**) Cells were left untreated or were transfected with NS or TS-1 siRNAs for 72 h, after which cell lysates were prepared and assayed for TS activity. Data are expressed as a percentage of the value for untreated cells and are means ± s.d. of triplicates from experiments that were repeated on at least one additional occasion with similar results. (**D**) Cells were left untreated or were transfected with NS or TS-1 siRNAs for 72 h, after which cell viability was assessed with the MTT assay. Data are expressed as a percentage of the value for untreated cells and are means of triplicates from experiments that were repeated on two additional occasions with similar results. (**E**) Cells were left untreated or were transfected with NS or TS-1 siRNAs for the indicated times, after which cell viability was assessed with the MTT assay. Data are means ± s.d. of triplicates from experiments that were repeated on two additional occasions with similar results.

and inhibitor of apoptosis (IAP) families of proteins, both of which are important regulators of apoptotic signalling pathways (Hengartner, 2000). Although depletion of TS did not substantially affect the expression levels of Bcl-2, Bcl-x_L, Bax, Bak, and survivin, it resulted in a substantial decrease in the abundance of X-linked inhibitor of apoptosis (XIAP) (Figure 5A). The activity of XIAP is